

Review

Recent Progress in Asymmetric Catalysis and Chromatographic Separation by Chiral Metal–Organic Frameworks

Suchandra Bhattacharjee, Muhammad Imran Khan, Xiaofang Li, Qi-Long Zhu *  and Xin-Tao Wu

State Key Laboratory of Structural Chemistry, Fujian Institute of Research on the Structure of Matter, Chinese Academy of Sciences, Fuzhou 350002, China; suchandra@fjirsm.ac.cn (S.B.); raoimranishaq@fjirsm.ac.cn (M.I.K.); lixiaofang@fjirsm.ac.cn (X.L.); wxt@fjirsm.ac.cn (X.-T.W.)

* Correspondence: qlzhu@fjirsm.ac.cn; Tel.: +86-591-63173129

Received: 7 February 2018; Accepted: 15 March 2018; Published: 19 March 2018

Abstract: Metal–organic frameworks (MOFs), as a new class of porous solid materials, have emerged and their study has established itself very quickly into a productive research field. This short review recaps the recent advancement of chiral MOFs. Here, we present simple, well-ordered instances to classify the mode of synthesis of chiral MOFs, and later demonstrate the potential applications of chiral MOFs in heterogeneous asymmetric catalysis and enantioselective separation. The asymmetric catalysis sections are subdivided based on the types of reactions that have been successfully carried out recently by chiral MOFs. In the part on enantioselective separation, we present the potentiality of chiral MOFs as a stationary phase for high-performance liquid chromatography (HPLC) and high-resolution gas chromatography (GC) by considering fruitful examples from current research work. We anticipate that this review will provide interest to researchers to design new homochiral MOFs with even greater complexity and effort to execute their potential functions in several fields, such as asymmetric catalysis, enantiomer separation, and chiral recognition.

Keywords: chiral metal–organic frameworks; chiral ligand; asymmetric catalysis; enantioselective separation

1. Introduction

Metal–organic frameworks (MOFs), as a unique class of coordination polymers, exist as well-organized crystalline structures and exhibit varied coordination geometries [1–4]. The diversity of metals and organic bridging ligands offers numerous structural and functional variations of MOFs, and directs the materials to various promising applications, such as catalysis [5–7], gas storage [8,9], chromatographic separation [10–12], chemical sensing [13–16], membranes [17,18], and drug delivery [19,20]. Considering the importance of chirality, today, research work on chirality has been expanded to numerous fields [21–23]. One of the most actively emerging fields is the design and synthesis of chiral MOFs [24] and exploring their applications in various fruitful research fields, including asymmetric catalysis [25–28], molecular recognition [29], non-linear optics [30–32], and enantioselective separation [33,34]. Several structural features of chiral MOFs, such as their large internal surface area, high adsorption capacity, efficient porosity, chemically and thermally stable skeleton, and above all chiral atmosphere, play a vital role in performing the above-mentioned applications (Figure 1). However, the successful design and application of chiral MOFs are challenging tasks for researchers. The present review outlines the recent applications in asymmetric catalysis and chiral separation explored by chiral MOF.

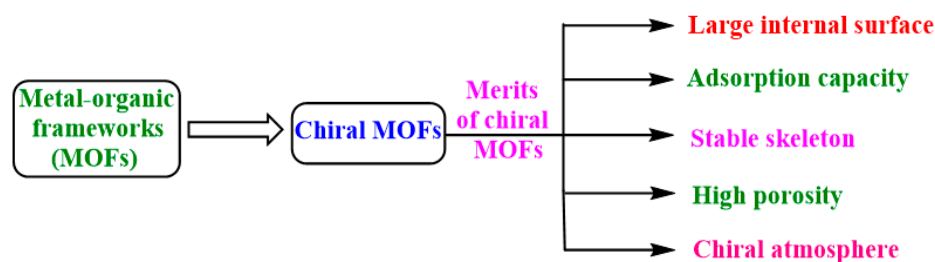


Figure 1. Typical structural requirement for chiral MOFs for their applications.

Asymmetric catalysis [25] is one of the essential areas of chiral chemistry, which efficiently assists the synthesis of valuable chiral products by selectively making and breaking the chemical bonds in an organic transformation. From the economic and ecological point of view, the use of homochiral MOFs as asymmetric catalysts is considered to be a potential eco-friendly method due to their numerous advantages, including mild reaction conditions, high enantiomeric excess, easy purification of the products, and reusability of the catalysts. Moreover, the reactions can take place in the inner pores of a chiral MOF catalyst, which serve as reaction chambers to facilitate the guest molecules to access the catalytically active sites within the pores. The size of the pores can be changed by changing the linkers of the MOFs. Due to these numerous benefits of homochiral MOF catalysts, a wide variety of chiral MOFs have been designed and explored as asymmetric catalysts. Consequently, the field has expanded rapidly and chiral MOF chemistry has been developing remarkably.

Chiral MOFs also provide a significant role for enantioselective separation [10,11]. As we know, the separation of chiral isomers is a challenging task because of their identical physical and chemical properties. A chiral environment is required to separate the chiral isomers as the different affinities grasped by the chiral isomers have different spatial structures. A large number of chiral stationary phases based on crown ethers, polysaccharides, glycopeptides, and proteins have been reported for the separations of chiral isomers [35–37]. Alternatively, chiral MOFs are regarded as prospective chiral stationary phases in HPLC and GC for enantioselective separation. The main advantages of chiral MOFs over other chiral stationary phases are their well-ordered frameworks containing available chiral pores to interact with guests and their controllable functionalities by varying chiral linkers and metal ions as the separation isomers require. Therefore, the selectivity and the separation of chiral isomers can be efficiently done by chiral MOFs.

Quite a few review articles have appeared recently on chiral MOFs [38–41]. The reviews have endeavored to describe the synthesis of those chiral MOFs that are suitable for applications in various fields. As this field is advancing rapidly, a new review article to provide an overview of the recent progress in applications of chiral MOFs is quite necessary. This review article is primarily divided into two parts. The first part mainly focuses on the emerging synthetic strategies for obtaining chiral MOFs and the second part highlights the recent successful applications of chiral MOFs from 2014 in the fields of asymmetric catalysis and chromatographic separation. Each part of the review is subdivided based on the synthetic approaches to chiral MOFs, the type of reactions carried out, and the different methods used for chromatographic separation, aiming to facilitate readers to understand them easily. We envision that this brief overview will provide researchers with means to catch up straightforwardly with recent advancement in the research on chiral MOFs.

2. Synthetic Strategies of Chiral MOFs

Chiral MOFs can be built by using numerous distinct strategies, each of which has its individual advantages and disadvantages [42,43]. In this review, we have classified the synthesis of chiral MOFs broadly into two different classes, namely the straightforward method and the indirect method, which are based on the component used for creating chirality within MOFs. The straightforward method for constructing chiral MOFs uses chiral components, such as enantiopure ligands or chiral salen, to react

with metal salts, where the chirality is directly created to the frameworks from the chiral components. In the indirect method, achiral bridging ligands are used to synthesize achiral MOFs, which are subsequently transferred to chiral MOFs by applying various techniques, such as (a) post-synthetic modification (PSM) by reacting an achiral MOF with a chiral auxiliary and (b) a superficial chiral etching process (SCEP); chiral MOFs can also be attained from achiral bridging ligands by the method called (c) spontaneous resolution and (d) chiral induction. Chiral induction can be done by using the appropriate chiral templates, namely, (i) a chiral-co-ligand or chiral spectator; (ii) a chiral-solvent, and (iii) circularly polarized light. Figure 2 presents the classification of the synthetic strategies of chiral MOFs.

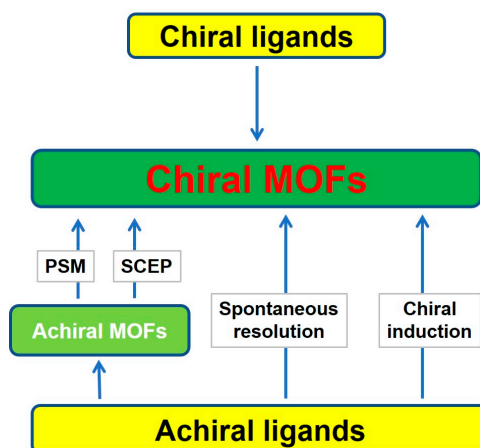


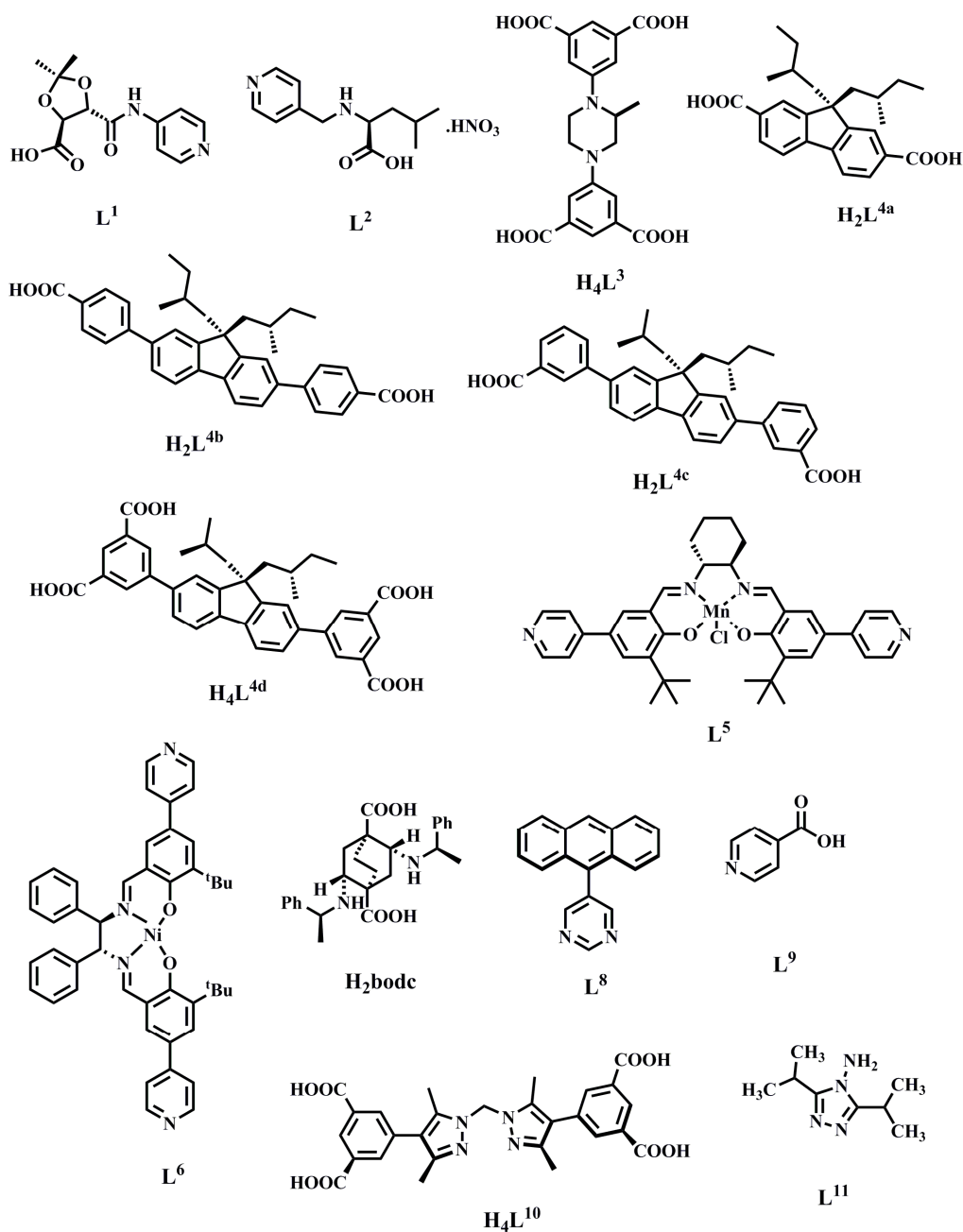
Figure 2. Schematic representation of the classification of the synthetic strategies of chiral MOFs. SCEP: superficial chiral etching process.

2.1. Straightforward Method

2.1.1. Chiral MOFs Prepared from Chiral Ligands

The conventional synthetic strategy for obtaining chiral MOFs greatly relies on chiral ligands (Scheme 1), in which the crucial step is the selection of suitable chiral ligands. In 2000, Kim and co-workers reported the synthesis of chiral MOFs from the enantiopure tartaric-acid-derived bridging ligands, $[\text{Zn}_3(\mu_3\text{-O})(\text{L}^1)_6]\cdot 2\text{H}_2\text{O}\cdot 12\text{H}_2\text{O}$ (**1**) ($\text{L}^1 = (4S,5S)\text{-}2,2\text{-dimethyl-}5\text{-pyridine-4-ylcarbamoyl-}1,3\text{-dioxolane-4-carboxylic acid}$) [44]. Subsequently, the method has been developed, and many research papers have been reported that use naturally occurring enantiopure amino acids and their derivatives [45–48], tartaric acid derivatives [49,50], and modified 1,1'-binaphthalene-2,2'-diol (BINOL) derivatives [51–53] for designing chiral MOFs. Recently, the approach of synthesis has been extended widely with some alteration, which will be described in the review.

Duan and coworkers [54] in 2015 described the synthesis of two new chiral polyoxometalate (POM)-based MOFs. The one-pot solvothermal reaction of chiral ligands *L*- and *D*-*N*-tert-butoxycarbonyl-2-(imidazole)-1-pyrrolidine (*L*-BCIP/*D*-BCIP), $\text{Zn}(\text{NO}_3)_2\cdot 6\text{H}_2\text{O}$, the bridging ligands NH_2 -bipyridine, and the Keggin-type $[\text{ZnW}_{12}\text{O}_{40}]^{6-}$ oxidation catalyst fruitfully furnished chiral POM-based MOFs denoted as ZnW-PYI1 (**2a**) and ZnW-PYI2 (**2b**), respectively. The synthesized ZnW-PYI can act as an efficient asymmetric catalyst for the conversion of carbon dioxide to cyclic-carbonates on reacting with olefins. The catalyst becomes highly stereoselective as the oxidant $[\text{ZnW}_{12}\text{O}_{40}]^{6-}$ and the *L*-BCIP ligands in the pores control the alignment of the substrate moieties in the reaction medium. Figure 3 presents the synthetic mode of the homochiral MOF and its catalytic application in asymmetric reaction.



Scheme 1. Ligands commonly used for the synthesis of chiral MOFs.

In 2016, Kuang et al. [55] designed the chiral ligand *N*-(4-pyridylmethyl)-*L*-leucine HNO₃ (HL²·HNO₃) for preparing a homochiral MOF, [CdL²Br]·H₂O (3), and reported, for the first time, the helical arrangement of Ag nanoparticles (NPs) on this chiral MOF, denoted as h-Ag NPs@MOF (3). When the synthesized homochiral MOF (3) is soaked in AgNO₃ solution, the Ag(I) positive ions can slowly remove the weak auxiliary ligand Br(I) ions from the MOF, forming AgBr on the surface of the MOF. The successive reduction led to the formation of highly ordered Ag NPs. The h-Ag NPs@MOF was further studied and found that it can serve as a surface-enhanced Raman scattering (SERS) sensor for the enantioselective recognition of *D/L*-cysteine and *D/L*-asparagine enantiomers.

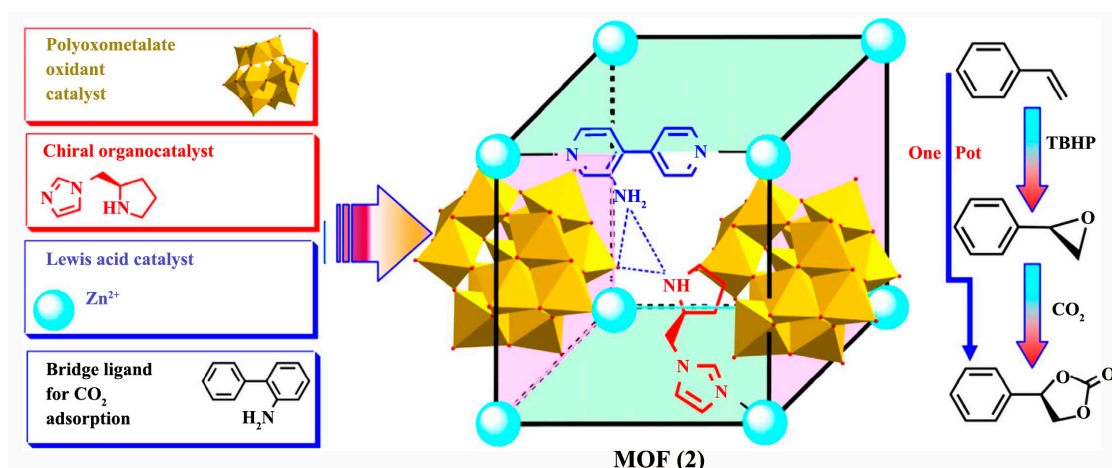


Figure 3. Synthetic procedure of the homochiral MOF ZnW-PYI (2) and schematic representation of the catalytic synthesis of cyclic-carbonates. Reproduced from [54] with permission from Nature Publishing Group.

In 2017, Li et al. [56] reported a series of homochiral zeolitic MOFs by employing four enantiopure amino acids (*L*-alanine (*L*-Ala), *D*-alanine (*D*-Ala), *L*-serine (*L*-Ser), and *L*-valine (*L*-Val)) with a 5-methyltetrazole (5-Hmtz) ligand, giving rise to four isostructural components, $[Zn_4(5\text{-mtz})_6(L\text{-Ala})_2]\cdot 2\text{DMF}$ (**4a**), $[Zn_4(5\text{-mtz})_6(D\text{-Ala})_2]\cdot 2\text{DMF}$ (**4b**), $[Zn_4(5\text{-mtz})_6(L\text{-Ser})_2]\cdot 2\text{DMF}$ (**4c**), and $[Zn_4(5\text{-mtz})_6(L\text{-Val})_2]\cdot 2\text{DMF}$ (**4d**), respectively (Figure 4). All four components showed permanent porosity with excellent enantioselective recognition capability.

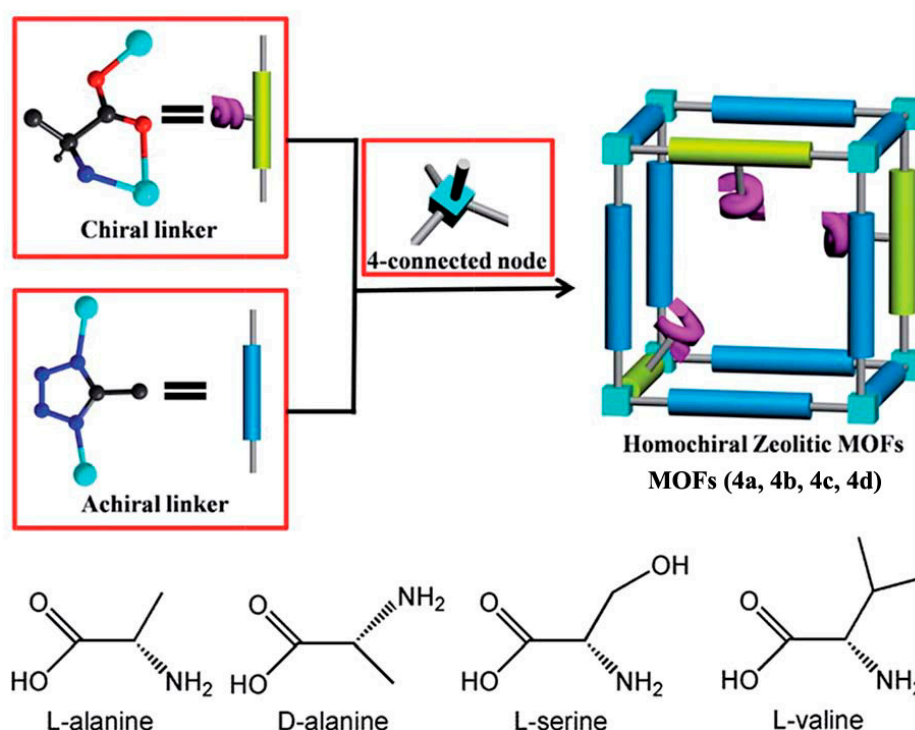


Figure 4. The synthetic strategies of homochiral zeolitic MOFs **4a**, **4b**, **4c**, and **4d**. Reproduced from [56] with permission from the Royal Society of Chemistry.

Bharadwaj and co-workers [57] recently designed a chiral tetracarboxylic acid ligand, 5,5'-[(S)-(+)-2-methylpiperazine-1,4-diyl]-diisophthalic acid (H_4L^3), and utilized the ligand to construct the homochiral MOF $[Cu_2(L^3)(H_2O)] \cdot 4DMF \cdot 4H_2O$ (**5**) under solvothermal conditions. The MOF (**5**) displayed high catalytic activity in an A^3 coupling reaction and a Pechmann reaction for the synthesis of imidazopyridine and coumarin derivatives, respectively. Yaghi and co-workers [58] reported the first instances of two Ca-based MOFs from naturally occurring nontoxic lactate linkers, $[Ca_{14}(L\text{-lactate})_{20}(\text{acetate})_8(C_2H_5OH)(H_2O)]$ (MOF-1201; (**6a**)) and $[Ca_6(L\text{-lactate})_3(\text{acetate})_9(H_2O)]$ (MOF-1203; (**6b**)), respectively, and subsequently demonstrated that MOF-1201 served as a degradable carrier for pesticides. By varying the position and/or number of carboxylate functions attached to the fluorenyl moiety (H_2L^{4a} , H_2L^{4b} , H_2L^{4c} , H_2L^{4d}), four optically pure chiral Cu-based MOFs with diverse topologies have been synthesized and studied by Robin et al. [59]. Kaskel group [60] described a homochiral MOF, DUT-129 (DUT: Dresden University of Technology, (**7**)), based on zinc ions and a novel enantiopure H_2bdc (bicyclo[2.2.2]octane-1,4-dicarboxylate) linker containing chiral secondary amines and multiple stereocenters.

2.1.2. Chiral MOFs from Chiral Salen Ligands

Another direct approach to synthesize chiral MOFs is from metallosalen ligands (Scheme 1). Metallosalen ligands possess a huge size, which facilitates the synthesis of chiral MOFs with extra-large cavities. Consequently, the frameworks are highly stable towards water and heat and can bear harsh chemical environments, which leads them to expand their range of applications.

In 2006, Cho et al. [61] prepared metallosalen ligands with the pyridyl-substituted salen-manganese complex, N,N' -bis(3-tert-butyl-5-(4-pyridyl)-salicylidene)[(*R,R*)-1,2-cyclohexanediamine] $Mn^{III}Cl$ (L^5), and offered a chiral MOF with the robust pillared layer structure of $[Zn_2(bpdc)_2L^5] \cdot 10DMF \cdot 8H_2O$ (**8**), (H_2bpdc = 4,4'-biphenyldicarboxylic acid). The MOF (**8**) served as an efficient catalyst in an enantioselective epoxidation reaction. Since then, many research groups have made great efforts to synthesize chiral MOFs from metallosalen ligands [62,63].

Recently, in 2017, the highly stable chiral metallosalen-based MOF material, $[(Cu_4I_4)_2L^6_4] \cdot 20DMF \cdot 3CH_3CN$ (**9**), was successfully synthesized from CuI and a predesigned nickel(salen) ligand (L^6) [L^6 = (*R,R*)- N,N' -bis(3-tert-butyl-5-(4-pyridyl)salicylidene)-1,2-diphenylethylenediamine nickel(II)] by Li et al. The authors stated that the framework displays a rare (4 + 4) 8-fold interpenetrated structure with four-connected cubic Cu_4I_4 cluster nodes and two-connected Ni(salen) linkers. Despite 8-fold interpenetration, the structure possesses two types of one dimensional (1D) channels with large pore size. Additionally, as a heterogeneous catalyst, the chiral salen-based MOF has successfully catalyzed the cycloaddition reactions of carbon dioxide, azides, and alkynes with epoxides. Notably, the catalyst can be reused for three successive cycles without substantial loss of its structural integrity [64].

Another noteworthy development was the fruitful synthesis of multivariate MOFs (MTV-MOFs), where one, two, or three different enantiopure metallosalen organic linkers were strategically placed and combined into one single framework. The metallosalen-derived ligands H_2L^{7M} (M = Cu, VO, CrCl, MnCl, Fe(OAc), and Co(OAc)) were first prepared by carrying out the reaction with N,N' -bis(3-tert-butyl-5-(carboxyl)salicylide) (H_4L^7) and the corresponding metal salts in MeOH. Next, five binary MTV-MOFs (**10**) (CuV, CuCr, CuMn, CuFe, and CuCo) were prepared by heating a 1:1 mixture of H_2L^{7M} (M = VO, CrCl, MnCl, Fe(OAc), Co(OAc)) and H_2L^{7Cu} with $Zn(NO_3)_2 \cdot 6H_2O$ in N,N -Dimethylformamide (DMF) and MeOH at 80 °C. The authors also successfully prepared two crystals of the ternary MTV-MOFs (CuMnCr and CuMnCo) by using a similar strategy (Figure 5). The synthesized MTV-MOFs (**10**) are efficient heterogeneous asymmetric catalysts for many enantioselective reactions, which will be discussed in the asymmetric catalysis sections of the review [65].

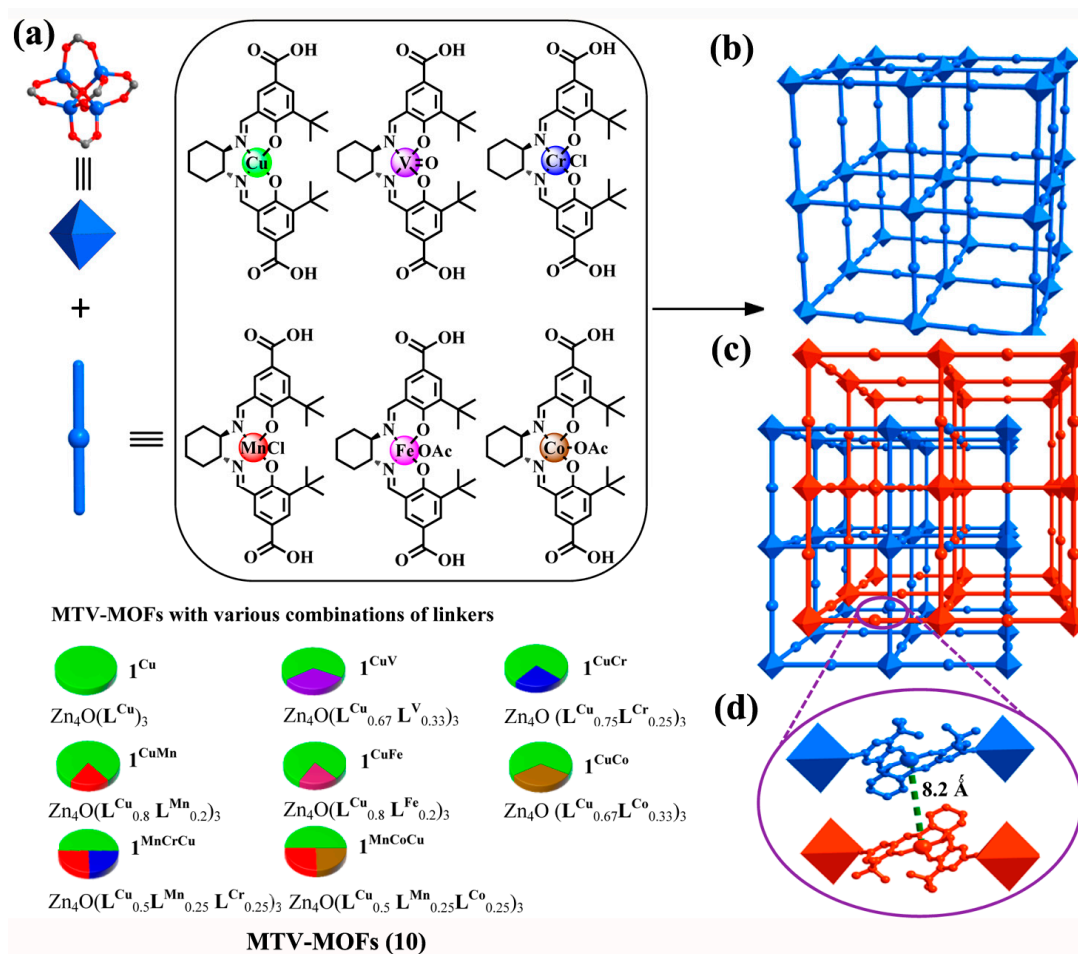


Figure 5. (a) Construction of MOF 10^{Cu} and corresponding multivariate (MTV)-MOFs 10^{CuM} and 10^{CuMM} with different metallosalen linkers; (b) one three-dimensional (3D) unit of MOF 10^{CuM} ; (c) two-fold interpenetrating 10^{Cu} (red indicates the interpenetrated 3D network); (d) close-up view of two L^{Cu} units brought into proximity to each other by 2-fold interpenetration. Reproduced from [65] with permission from the American Chemical Society.

2.2. Indirect Method

2.2.1. Post-Synthetic Modification (PSM)

The PSM of previously synthesized MOFs is an efficient approach to produce chiral MOFs. The key fact for this method is the functional groups in the organic ligands of the pre-synthesized achiral MOFs, which are susceptible to react with the chiral reagents. This approach affords a means of decorating the MOFs with a variety of chiral functionalities, which may be impossible or tedious to synthesize through conventional routes.

Cohen and co-workers demonstrated that the amino groups of IRMOF-3 (IRMOF = isorecticular MOF) can be changed with amides by reacting them with enantiopure anhydride, resulting in the formation of chirality in the framework [66–69]. Bonnefoy et al. [70] designed novel MOFs to which are attached enantiopure peptide moieties. The three different MOFs, Al-MIL-101-NH₂ (**11a**), In-MIL-68-NH₂ (**11b**), and Zr-Uio-66-NH₂ (**11c**), were chosen to react under microwave irradiation with numerous oligopeptides (up to tetrapeptides) for the synthesis of chiral hybrid solids. The microwave irradiation controls the peptide racemization and offers a better grafting yield than the conventional methods for the reaction.

In 2016, Fröba and associates [47] reported the PSM of the oxazolidinone moieties connected to the MOF UHM-25-Val-Evans (**12**). The acylation of the MOF (**12**) was attained by reacting it with propionic anhydride in the presence of a nucleophilic catalyst 4-(dimethylamino)pyridine (DMAP) as shown in Figure 6. The reaction was initially stirred for 24 h, yielding 37% of *N*-acylated product. By increasing the reaction time from 24 h to 72 h, the rate of conversion can be further increased to 90%.

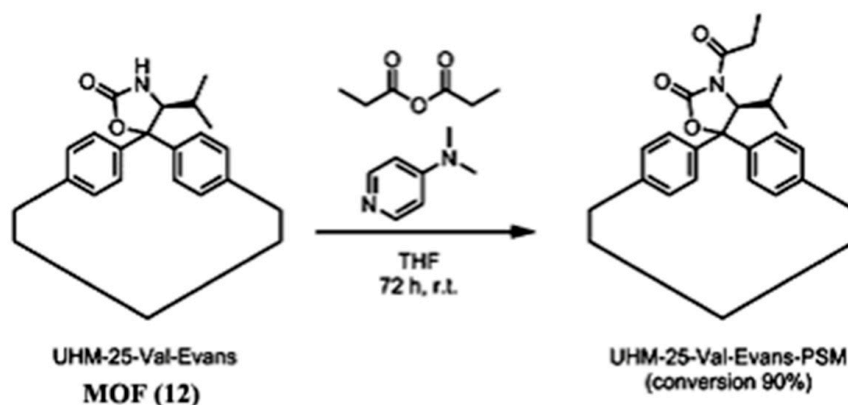


Figure 6. Post-synthetic acylation of UHM-25-Val-Evans (**12**). Reproduced from [47] with permission from the American Chemical Society. r.t.: room temperature.

Recently, Chen et al. [71] designed a chiral MOF, (*R,R*)-salen(Co(III))@IRMOF-3-AM (**13**), by using a two-step procedure. In the first step, the (*R,R*)-salen(Co(III)) metal complex was adsorbed in the nanocages of IRMOF-3, and in the second step, by PSM, the free amino groups present on IRMOF-3 were acylated by anhydride (Figure 7).

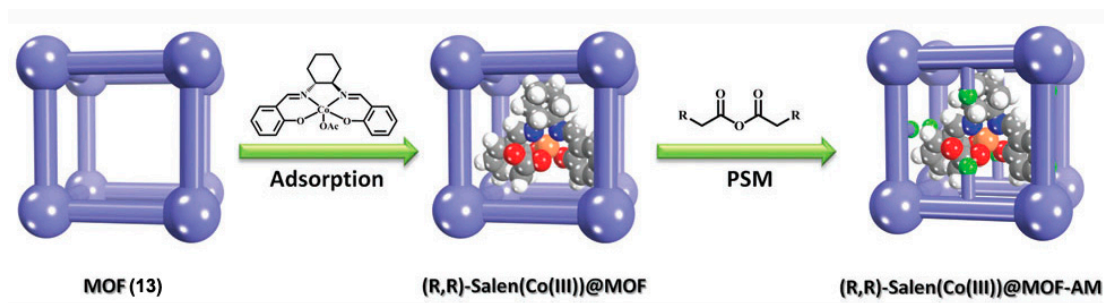


Figure 7. Synthetic method of (*R,R*)-salen(Co(III))@IRMOF-3-AM (**13**). Reproduced from [71] with permission from the Royal Society of Chemistry.

2.2.2. Superficial Chiral Etching Process

Hou et al. [72] recently designed chiral-achiral hybrid MOFs with the core-shell structure of an achiral MOF@homochiral MOF by employing a new technique called the superficial chiral etching process (SCEP). In this process, the surface of the pre-synthesized achiral MOF, $[\text{Cu}_3(\text{Btc})_2]$ (**14**), provides a Cu(II) source to react with (+)-Cam and Dabco to generate a homochiral MOF $[\text{Cu}_2((+)\text{-Cam})_2\text{Dabco}]$ (**15**) shell on the surface of the achiral MOF (**14**), leading to $[\text{Cu}_3(\text{Btc})_2]@[\text{Cu}_2((+)\text{-Cam})_2\text{Dabco}]$ (**16**). The synthesized MOF (**16**) demonstrated the enantioselective sorption of (*R*)- and (*S*)-limonene (Figure 8).

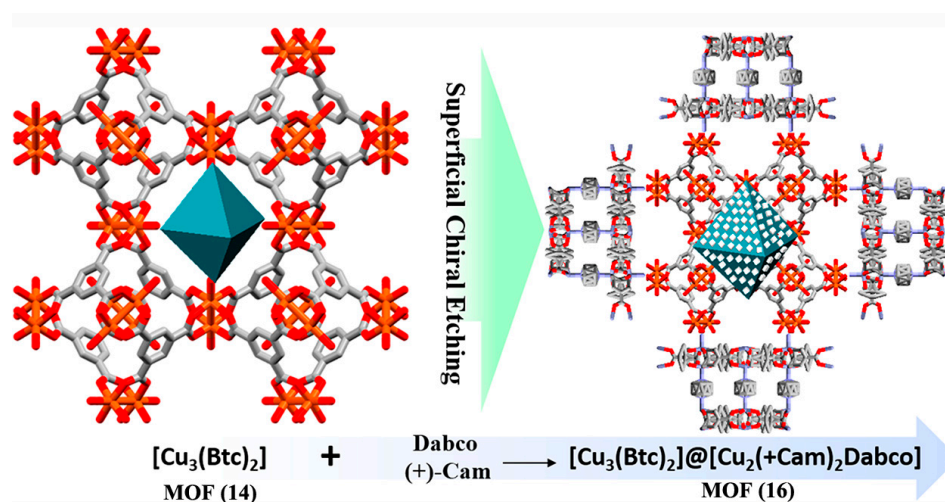


Figure 8. Schematic representation of the superficial chiral etching process for MOF 16. Reproduced from [72] with permission from the American Chemical Society.

2.2.3. Spontaneous Resolution

In this method, chiral MOFs are built from achiral precursors through crystallization in the enantiomorphous space group within the MOFs. During crystallization, it breaks its symmetry for spatial organization and thus helps to produce chiral MOFs. Such a type of self-resolution process is very common and contains both types of enantiomers, resulting in a racemic mixture.

Aoyama and co-workers [73] were the first to establish that homochiral MOFs can be achieved through self-crystallization. They reported an enantiomerically pure MOF, $[\text{Cd}(\text{L}^8)(\text{NO}_3)_2(\text{H}_2\text{O})(\text{EtOH})]$ (17) ($\text{L}^8 = 5$ -(9-anthracenyl)pyrimidine), created due to the twisted arrangement of the pyrimidine group with respect to the anthracene moiety during crystallization. Li et al. [74] reported a chiral porous MOF, $[\text{Co}_6(\mu_3\text{-OH})_2(\text{IN})_4(\text{HCOO})_6] \cdot 4\text{DMF} \cdot 5\text{H}_2\text{O}$ (18), from the solvo(hydro) thermal reactions of achiral isonicotinic acid (HIN) (HL^9) with $\text{Co}(\text{NO}_3)_2 \cdot 6\text{H}_2\text{O}$. The IN^- ligands associated with the adjacent 1D secondary building units (SBUs) resulted in a three-dimensional (3D) chiral MOF with a pcu framework containing irregular channels. A few more new studies on spontaneous resolution have been reported [75–79].

Bharadwaj and co-workers [80] recently designed a thermally stable cadmium-based chiral MOF from an achiral v-shaped ligand by spontaneous resolution. The synthesis of bis[4-(3,5-dicarboxyphenyl)-1H-3,5-dimethylpyrazolyl] methane (L^{10}) was accomplished in five steps using acetylacetone as the starting material. The solvothermal reaction of $\text{Cd}(\text{NO}_3)_2$ with L^{10} in DMF/water led to the formation of $[\text{Cd}_2(\text{L}^{10})(\text{H}_2\text{O})(\text{DMF})] \cdot 3\text{DMF} \cdot 2\text{H}_2\text{O}$ (19) with a unique 3,6-conn topology. The authors stated that the metal ions coordinate with the ligand L^{10} , which restricts the rotation of the ligands and results in the chiral network from the selective and directional coordination of metal ions. Moreover, the synthesized chiral MOF was applied as a catalyst in a three-component Strecker reaction with a high conversion yield.

2.2.4. Chiral Induction

An approach to synthesize chiral MOFs is the use of chiral additives that are capable of inducing achiral precursors to generate homochiral MOFs. Common chiral additives are chiral ionic liquid, chiral co-agents, and chiral spectators, which are usually not the building blocks of the MOFs, but assist the MOFs to be chiral. Such chiral induction remains unstated, but the greatest advantage is that the method is cost-effective and not limited to any linkers. The key step for this approach is the selection of chiral induction agents for a given set of precursors.

Morris and co-workers [81] primarily revealed the induction of homochirality in the MOF (BMIm)₂[Ni(Hbtc)₂(H₂O)₂] (**20**) by a chiral ionic solvent used as a reaction medium containing 1-butyl-3-methylimidazolium *L*-aspartate (BMIm-*L*-asp). A further study of this mode of synthesis lead to the growth of the concept of using chiral co-agents during the synthesis of MOFs [82–84].

In 2015, Zaworotko and associates [85] demonstrated that MOF-5 can be easily changed to the chiral variants Λ -CMOF-5 (**21a**) and Δ -CMOF-5 (**21b**) through chiral induction by using additive *L*-proline or *D*-proline during synthesis. The alteration of the backbone of the MOF-5 leads to the formation of CMOF-5, which further crystallizes in the chiral cubic space group P2₁3. A new achiral compound, [Zn(BDC)(NMP)], was formed in absence of *L*-proline or *D*-proline, indicating that the presence of proline is vital for the crystallization of Λ -CMOF-5 or Δ -CMOF-5. The authors also verified the post-synthetic activity of the achiral solvent *N*-methyl-2-pyrrolidone (NMP), and surprisingly found that in both cases of CMOF-5 as well as MOF-5, the presence of NMP offered a racemic conglomerate of CMOF-5, whereas other organic solvents transformed CMOF-5 into MOF-5 (Figure 9).

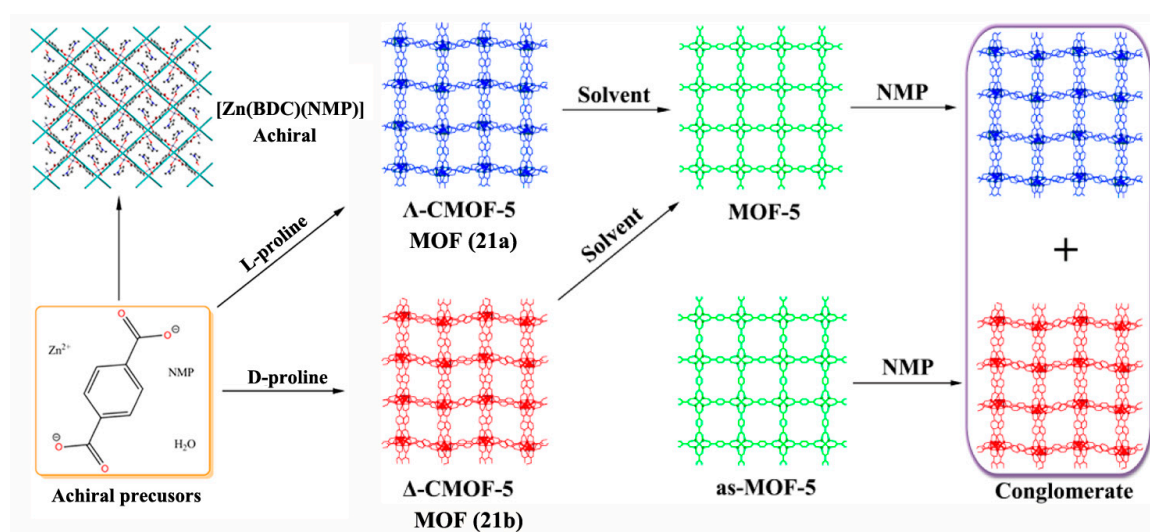


Figure 9. Synthesis of CMOF-5 in the presence of *L*- or *D*-proline additives induces chirality and post-synthetic activity of the achiral solvent *N*-methyl-2-pyrrolidone (NMP). Reproduced from [85] with permission from the American Chemical Society.

Li et al. [86] showed the effect of ionic liquid on the synthesis of chiral MOFs, where they designed two 3D MOFs, [Th(TPO)(OH)(H₂O)]·8H₂O (**22a**) and [C₉H₁₇N₂][Th(TPO)Cl₂] (**22b**), from the same achiral starting materials by applying solvothermal and ionothermal methods, respectively. The solvothermal method resulted in a centrosymmetric MOF **22a**, whereas, in the ionothermal reaction, chiral MOF **22b** was obtained by using the ionic liquid 1-butyl-2,3-dimethylimidazolium chloride. Recently, Su and co-workers [87] constructed an enantiomeric pair of three-dimensional MOFs [Cu₄(L¹¹)₃(NO₃)₃]·3H₂O (**23**) from the achiral ligand L¹¹ (L¹¹ = 3,5-diisopropyl-1,2,4-triazolate) by using *L*-amino acid and *D*-amino acid as the chiral catalysts, respectively. From a crystallographic study and elemental analysis, it was found that the enantiopure amino acids were not anchored into the final crystal structures of the MOFs. By exchanging *L*-/*D*-amino acids with lactic acid or mandelic acid, the authors successfully proved the mechanism of chirality induction. It was noted that lactic acid and mandelic acid were inefficient chiral inducers for this set of precursors, which illustrates that the OH groups of lactic acid and mandelic acid have a weaker affinity to Cu ions than do the NH₂ groups of *L*-/*D*-amino acids. NH₂ groups of *L*-/*D*-amino acids firstly bind with Cu ions and are further substituted by achiral ligands to arrange themselves in 3D chiral frameworks (Figure 10).

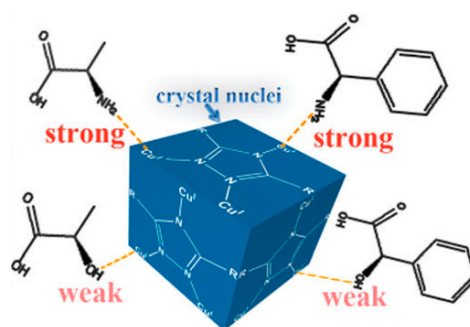


Figure 10. The plausible mechanism of the chiral induction effect. Reproduced from [87] with permission from the Royal Society of Chemistry.

An exciting report was presented by Wu et al. [88], where a chiral MOF, [Cu-(succinate)(4,4'-bipyridine)]·4H₂O (**24**), was constructed from achiral precursors and the chirality in the MOF was initiated by using the irradiation of circularly polarized light (CPL) during the crystallization. After investigating 92 samples, the authors concluded that CPL irradiation can provide enantiomeric excess and a left-handed helical structure was attained by left-handed CPL irradiation during the reaction or crystallization, and a right-handed helical structure was achieved with right-handed CPL irradiation.

Thus, we have described several new approaches recently explored for the construction of chiral MOFs, which will certainly offer new opportunities to researchers for synthesizing bulk homochiral MOFs.

3. Applications of Chiral MOFs

3.1. Asymmetric Catalysis

In the field of heterogeneous catalysis, chiral MOFs can be used as outstanding solid catalysts for many organic reactions, including enantioselective reactions, which cannot be accomplished by the conventional heterogeneous catalysts. The porosity, structural stability, and reusability of chiral MOFs make them highly demanded chiral catalysts for large-scale organic transformations. Some of the recent innovative works on enantioselective reactions are endorsed by chiral MOFs and will be briefly described in the review. This part is subdivided based on the reactions catalyzed by chiral MOFs.

3.1.1. 1,4-, 1,2-, and Cyclo-Addition Reactions

Lin and co-workers [89] extensively explored the catalytic activities of metal-based homochiral MOFs in a varied range of asymmetric organic transformations. The post-synthetically prepared Rh- and Ru-complex-based BINAP-derived chiral MOFs offered high enantioselectivity for a variety of asymmetric reactions. The BINAP-derived dicarboxylic acid, H₂L¹², was prepared by a multistep reaction starting from 4,4'-I₂-BINAP (Figure 11a). The chiral Zr-MOF was prepared from H₂L¹² and its post-synthetic metalation was done by treating [Zr₆O₄(OH)₄(L¹²)₆] (**25**) with [Rh(nbd)₂(BF₄)] to afford [Zr₆O₄(OH)₄(L¹²)₆]·Rh (**25a**) and with Ru(cod)(2-Me-allyl)₂ followed by HBr to afford [Zr₆O₄(OH)₄(L¹²)₆]·Ru (**25b**), respectively (Figure 11b). A 1 mol % volume of catalyst (**25a**) exhibited excellent enantioselectivity—up to >99%—in the 1,4-addition of aryl boronic acids to 2-cyclohexanone. Similarly, outstanding activity was showed by the same catalyst in 1,2-addition of AlMe₃ to α,β-unsaturated ketones to afford chiral allylic alcohols. Ru-functionalized MOF (**25b**) showed high activity in the hydrogenation of β-keto esters and substituted alkenes, with an ee of up to 97% and 91%, respectively.

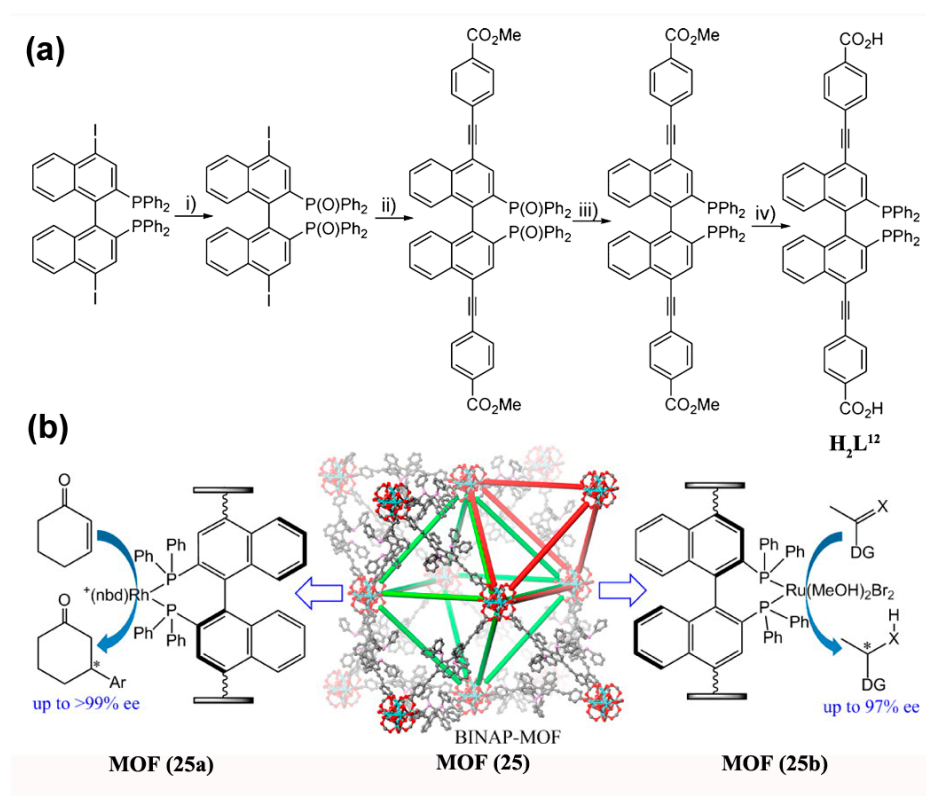
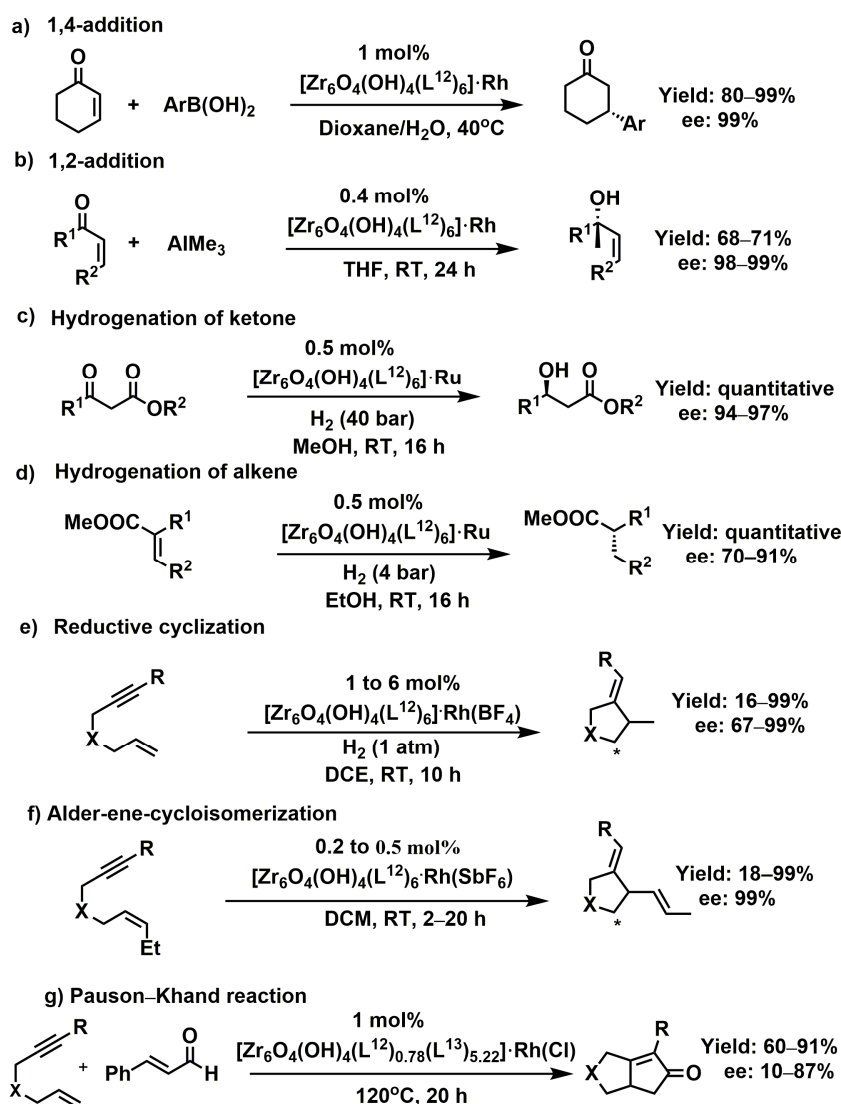


Figure 11. (a) Synthesis of the ligand H_2L^{12} . (b) Synthesis of homochiral MOFs by post-synthetic metalation of **25a** and **25b** and their applications in asymmetric catalysis. Reproduced from [89] with permission from the American Chemical Society.

Later, the same group [90] extended the scope of the BINAP-MOF.Rh catalyst and demonstrated good yield with high enantioselectivity—up to 99%—towards the asymmetric reductive cyclization and Alder-ene cyclo isomerization of 1,6-enynes for constructing cyclized products. The catalyst presented 4–7 times higher catalytic activity and enantioselectivity compared to the conventional homogeneous catalysts. However, the recovered BINAP-MOF.Rh catalyst showed low or no catalytic recyclability. The catalyst exhibited no activity towards sterically hindered asymmetric Pauson–Khand-type reactions. To overcome this problem, Lin and co-workers introduced a mixed ligand concept, for expanding the space near the catalytic sites, to accommodate the intermediates of the reaction, and successfully demonstrated Pauson–Khand-type reactions with 87% ee. The synthesized chiral MOF $[Zr_6(OH)_4O_4(L^{12})_{0.78}(L^{13})_{5.22}]$ (**26**) ($H_2L^{13} = 4,4'-((2\text{-nitro-[1,1'-binaphthalene]-4,4'-diyl})\text{bis(ethyne-2,1-diyl)})\text{dibenzoic acid}$) with mixed linkers was subsequently treated with $[RhCl(nbd)]_2$ to form $[Zr_6(OH)_4O_4(L^{12})_{0.78}(L^{13})_{5.22}] \cdot RhCl$ (**26a**). The modified catalyst (**26a**) showed 10 times higher catalytic activity than the homogeneous control catalyst. Scheme 2 summarizes the catalytic activities of BINAP-MOFs explored recently for organic transformation.

The chiral diene-based MOF catalyst $E_2\text{-MOF}(Zr_6(\mu_3\text{-O})_4(\mu_3\text{-OH})_4(L^{14})_6 \cdot 143\text{DMF} \cdot 109\text{H}_2\text{O})$ (**27**) was used to create two efficient catalysts, $E_2\text{-MOF} \cdot RhCl$ and $E_2\text{-MOF} \cdot Rh(acac)$, by post-synthetic metalation with Rh(I) complexes, which subsequently demonstrated high catalytic activity and enantioselectivity for 1,4-additions of arylboronic acids to α, β -unsaturated ketones and asymmetric 1,2-additions of arylboronic acids to aldimines (Figure 12) [91]. Both of the reactions were successful for a broad range of substrate moieties under identical reaction conditions. The catalyst $E_2\text{-MOF} \cdot Rh(acac)$ was reused seven times without the loss of yield, ee, and crystallinity.



Scheme 2. Asymmetric organic transformations catalyzed by BINAP-MOFs: (a) 1,4-addition reaction by MOF(25a), (b) 1,2-addition reaction by MOF (25a), (c) Hydrogenation of ketone by MOF (25b), (d) Hydrogenation of alkene by MOF (25b), (e) Reductive cyclization of 1,6-enynes, (f) Alder-ene-cycloisomerization of 1,6-enynes, (g) Pauson-Khand reaction catalyzed by MOF (26a).

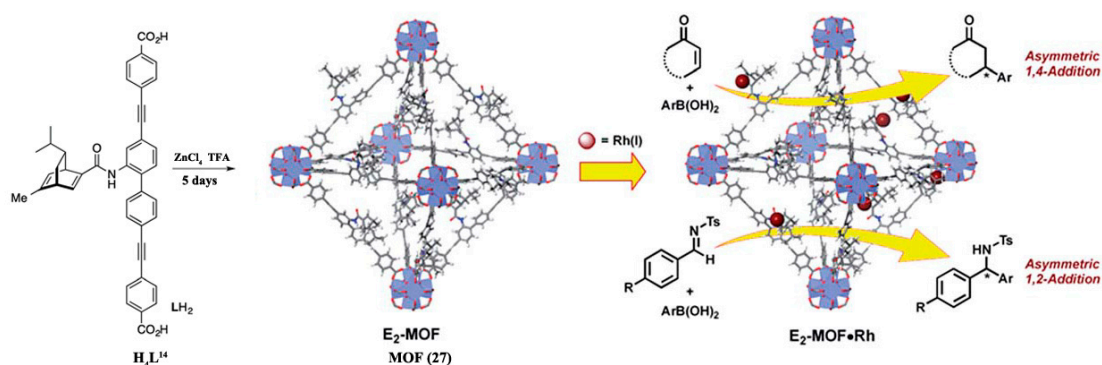
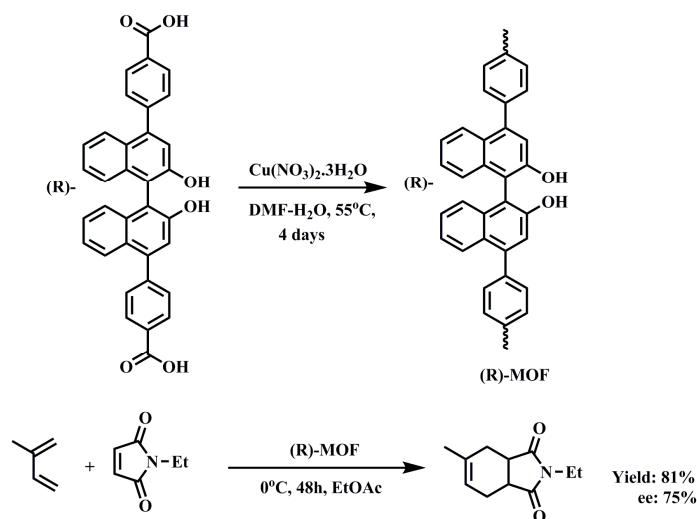


Figure 12. Synthesis of the homochiral E_2 -MOFs (27) from H_4L^{14} and its post-synthetic metalation and their application in asymmetric catalysis. Reproduced from [91] with permission from the Royal Society of Chemistry.

Jeong and co-workers [92] also described an Alder-ene cyclization reaction of 3,3,7-trimethyloct-6-enal facilitated by Zn/(*R*)-KUMOF-1 (**28**) with a high yield of 92% and 50% ee, respectively. The authors proved, with the experimental data, that the optical purity of the product depended on the crystal size and chiral environment of the voids of chiral MOFs.

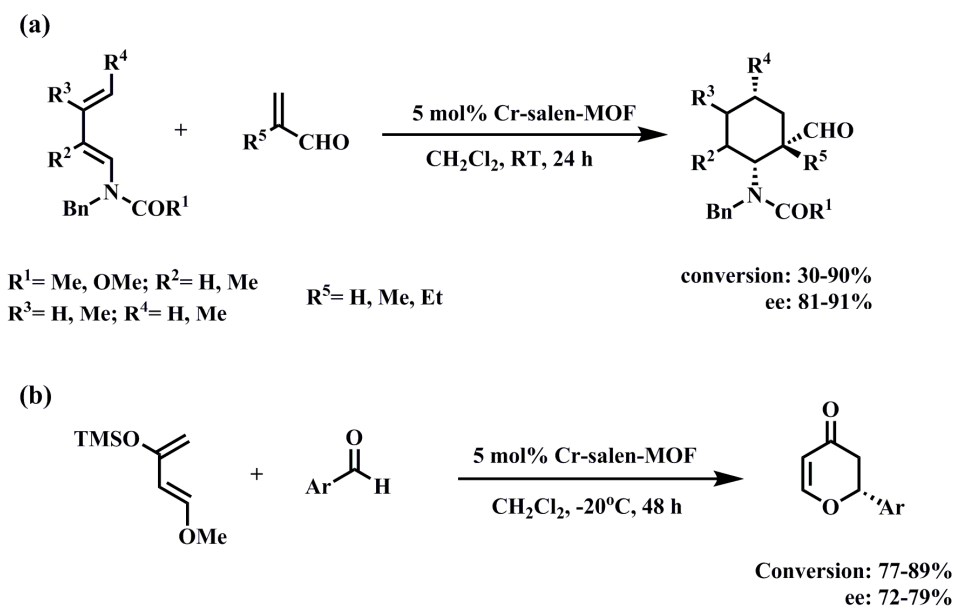
3.1.2. Diels–Alder Reaction

In 2016, Tanaka et al. [93] designed a novel homochiral biphenol-based MOF (**29**) from the solvothermal reaction of chiral organic ligand (*R*)-2,2'-dihydroxy-1,1'-binaphthyl-4,4'-dibenzoic acid (H_2L^{15}) and $Cu(NO_3)_2 \cdot 3H_2O$ in a mixed solvent (DMF– H_2O) at 55 °C for 4 days. The MOF crystallizes in the trigonal space group R32. The ligand H_2L^{15} was synthesized by Suzuki cross-coupling reaction of 4-methoxycarbonyl phenylboronic acid and (*R*)-4,4'-dibromo-2,2'-diacetyl-1,1'-binaphthyl followed by hydrolysis and acidification, respectively. The synthesized chiral MOF (**29**) was found to be an effective asymmetric catalyst in the Diels–Alder reaction between isoprene and *N*-ethyl maleimide, with up to 81% yield and 75% ee (Scheme 3). The optimized conditions for the reaction were explored and it was found that the best yield was obtained when the reaction was performed at 0 °C for 48 h in EtOAc solvent. The scope of the reaction was further studied with various *N*-substituted maleimides with isoprene, and lower reactivity and enantioselectivity were observed for bulky substrates due to their weak interactions with the synthesized chiral MOF.



Scheme 3. Diels–Alder reaction by chiral MOF (**29**).

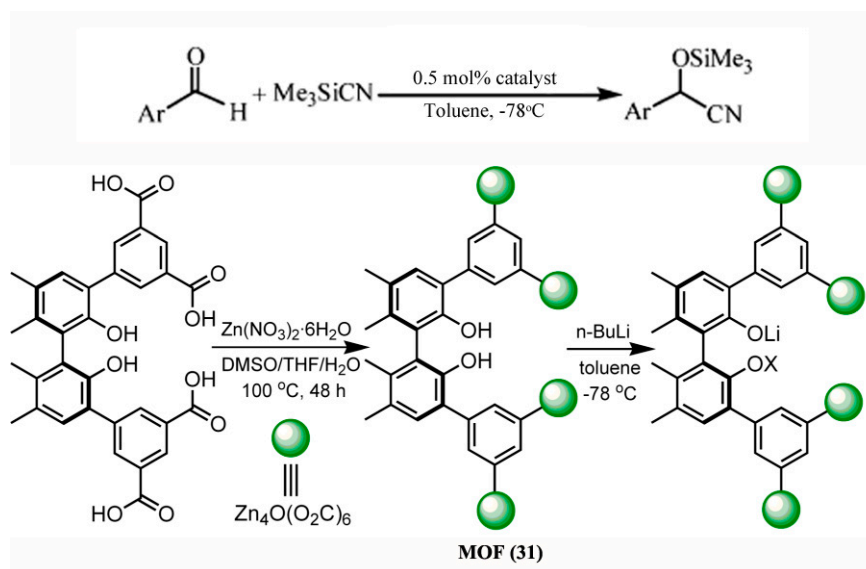
Cui and co-workers [94] designed a Cr(salen)-based MOF [$Na_5Cd_2(Cr\text{-salen})_4(OH)_2(O_2CCH_3)(O_2CH)_2(H_2O)_7(CH_3OH)_3 \cdot 12H_2O$] (**30**) and demonstrated its significant application as a catalyst for a variety of asymmetric organic transformations. The Diels–Alder reaction was explored with a range of methyl-substituted dienes, which successfully reacted with the substituted acrolein in the presence of 5 mol% of the synthesized MOF, affording the corresponding products in moderate conversions with an ee up to 91% (Scheme 4a). Similarly, the catalytic activity of the synthesized Cr(salen)-based MOF (**30**) in hetero-Diels–Alder reactions was also evaluated. The reactions proceeded smoothly with the substituted benzaldehydes and Danishefsky dienes, and the desired products were obtained with a conversion of 77–89% and 72–79% enantioselectivity after 48 h (Scheme 4b). The reaction afforded <5% conversion when a sterically hindered group was attached to the benzaldehyde moiety, indicating that a bulky substrate could not enter inside the MOF pores where the heterogeneous catalysis mainly occurred. Recently, the same group [65] described a Diels–Alder reaction with identical reactants using the MTV-MOF catalyst (*R*)-10^{CuCo}, which successfully afforded 88–94% ee of the cycloadducts.



Scheme 4. (a) Diels–Alder reaction and (b) Hetero-Diels–Alder reaction by a chiral Cr(salen)-based MOF (30).

3.1.3. Cyanosilylation of Aldehydes

Cui and co-workers [95] exemplified a homochiral biphenol-based MOF (31) with chiral dihydroxyl auxiliaries. These chiral dihydroxyl auxiliaries were partially exchanged by Li^+ ions and converted to a highly efficient and recyclable heterogeneous catalyst for the asymmetric cyanation of aldehydes with up to >99% ee (Scheme 5).



Scheme 5. Cyanation of aldehydes by a biphenol-based catalyst. Reproduced from [95] with permission from the American Chemical Society.

Later, the same group [96] illustrated the cyanation of aldehydes with two new chiral MOFs that were constructed from pairs of VO(salen) ligand for **32a**, and VO(salen) and Cu(salen) mixed ligands for **32b**. After oxidation with $(\text{NH}_4)_2\text{Ce}(\text{NO}_3)_6$, V(IV) centers in the pairs of VO(salen)-MOF (**32a**) were transformed to V(V) and the MOF became an effective catalyst for catalytic reactions,

with stereoselectivity up to >99%. The reaction offered better results with respect to conversion and enantioselectivity when the electron-donating group was attached with benzaldehydes compared to the presence of an electron-withdrawing group on the ring. Less than 5% conversion was obtained when a bulky aldehyde was used as a substrate. The MOF (**32b**) decorated with both VO(salen) and Cu(salen) units showed much lower reactivity and stereoselectivity compared to the VO(salen)-MOF (**32a**). This was due to the monometallic activation pathway that was observed in the MOF (**32b**), whereas a VO-VO cooperative activation mechanistic pathway was evidenced in the pairs of VO(salen)-MOF (**32a**) (Figure 13).

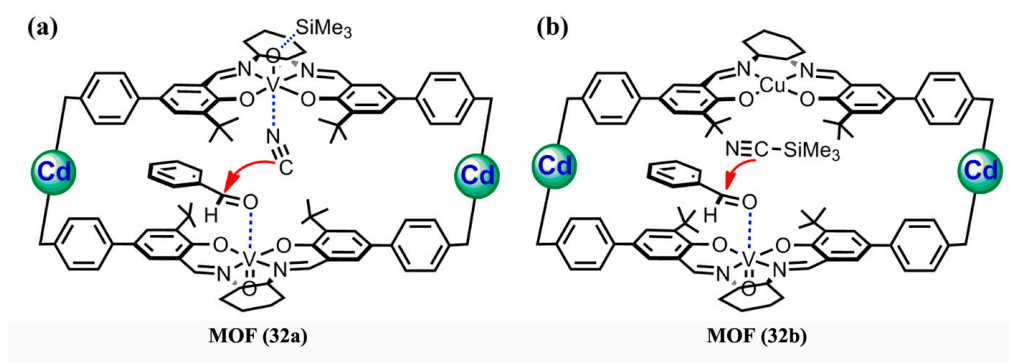


Figure 13. Proposed bimolecular (a) and unimolecular (b) activation pathways for the cyanation of aldehyde by **32a** and **32b**. Reproduced from [96] with permission from the American Chemical Society.

In 2017, Li et al. [97] constructed a novel porphyrin-salen-based chiral MOF by judiciously combining metalloporphyrin (tetra-(4-carboxyphenyl) porphyrin (H_6L^{16})) and metallosalen ((*R,R*)-*N,N'*-bis(3-tertbutyl-5-(4-pyridyl)salicylidene)-1,2-diphenyldiamine nickel(II) (NiL^{17})) struts into a chiral MOF structure of $[Cd_2(NiL^{17})(CdL^{16})][Cd_2(NiL^{17})(H_2L^{16})] \cdot 6DMF \cdot 5MeOH$ (**33**). The synthesized MOF acted as an efficient heterogeneous catalyst in the asymmetric cyanosilylation of aldehydes, and the reactions afforded excellent conversions of 81–96% and enantioselectivities of 55–98% for benzaldehyde and other aromatic aldehydes bearing electron-donating as well as electron-withdrawing groups. The conversion was radically decreased in the case of a bulky moiety, such as 9-anthraldehyde, suggesting that the selectivity and catalytic activity occurred inside the channels of the catalyst (**33**). The use of (*S*-) catalyst (**33**) afforded (*S*-) enantiomers as a product, which verified that the stereoselectivity of the products was directly controlled by the fundamental chiral nature of the catalyst.

3.1.4. Epoxidation of Alkenes and Cleavage of Epoxide Ring

The asymmetric epoxidation of alkenes and the corresponding ring opening of epoxides by MTV-MOFs were enlightened by Cui and co-workers [65]. The binary MTV-MOFs 10^{CuMn} and 10^{CuFe} were found to be active catalysts for the asymmetric epoxidation of alkenes, affording up to 93% and 90% ee of the epoxides with 89% and 94% conversion, respectively. After the success of the catalytic activity of binary MTV-MOFs, the tripartite MTV-MOFs (*R*)- 10^{CuMnCr} and (*R*)- 10^{CuMnCo} were also explored for the epoxidation of 2,2-dimethyl-2*H*-chromene and its derivatives, and the products were obtained with good conversion rates and high enantioselectivities. Similarly, the catalysts were further verified for the ring opening reaction of epoxides by the nucleophile aniline and water, but the enantioselectivities were less than 25% in both cases. Next, the consecutive reaction of the asymmetric epoxidation of alkene followed by ring-opening reactions of epoxides by various nucleophiles, such as aniline, $TMSN_3$, and $ArCH_2SH$, was explored successfully by employing the catalyst (*R*)- 10^{CuMnCr} . The various substituents on anilines had a slight effect on both the conversion and selectivity of the reactions, and overall the conversions obtained were 78–95% with an ee of 86–96%. A satisfactory

conversion (74–92%) with high enantioselectivity (84–99%) was achieved for azido alcohols derived from TMSN_3 . Similarly, a variation with benzyl mercaptan derivatives was also accompanied by suitable conversions (74–94%) and good to high enantioselectivities (86–99% ee). The heterogeneous catalyst (*R*)-**10**^{CuMnCo} confirmed its efficiency in the sequential reaction of epoxidation and cleavage of epoxide by nucleophile H_2O , alcohol, and ArCOOH . Later, the same group [98] constructed two other new binary MOFs by the cocrystallization of dipyridine and dicarboxylate-functionalized $\text{M}(\text{salen})$ complexes and demonstrated their efficiency as heterogeneous catalysts in the asymmetric sequential epoxidation of alkenes and epoxide ring-opening reactions.

Duan and associates [54] exemplified the fruitful catalytic activity of chiral ZnW-PYI (**2**) in the epoxidation of substituted styrenes with excellent yields (76–92%) and enantioselectivities (75–79%). After an effective transformation, the coupling of CO_2 to an (*R*) or (*S*)-styrene oxide was examined and showed an outstanding efficiency of conversion of >99% and high enantioselectivity of >90%. Chiral ZnW-PYI (**2**) proved its efficiency in the sequential one-pot transformation of olefins to cyclic carbonates via epoxide: 72–92% conversions and 55–80% enantioselectivities were obtained for sequential reactions with different substituted styrene derivatives. The author revealed that the hydrogen-bonding interactions between pyrrolidine-2-yl-imidazole (PYI) and the oxidation catalyst $\text{ZnW}_{12}\text{O}_{40}^{6-}$ and the π - π interactions between the benzene rings of styrene oxide and the imidazole rings of PYI prompted the smooth conversion of olefins into epoxides. In the case of cinnamaldehyde, only 25% conversion was obtained with zero ee under the same reaction conditions, which is due to the fact that the interactions of aldehyde groups with the NH_2 moieties deactivated sites for the activation of CO_2 molecules (Figure 14).

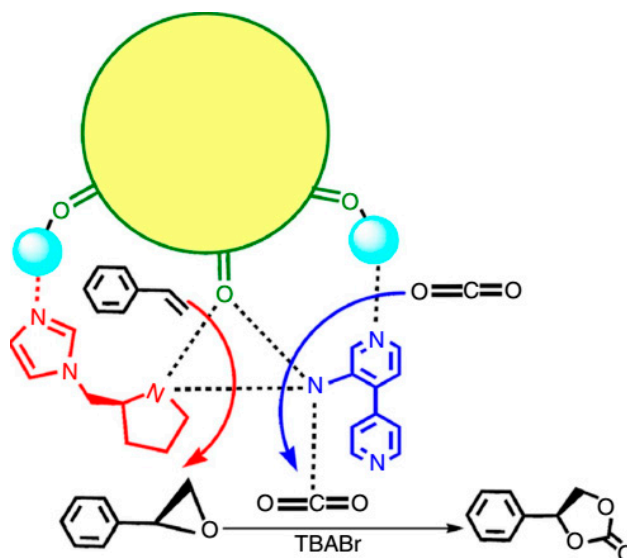


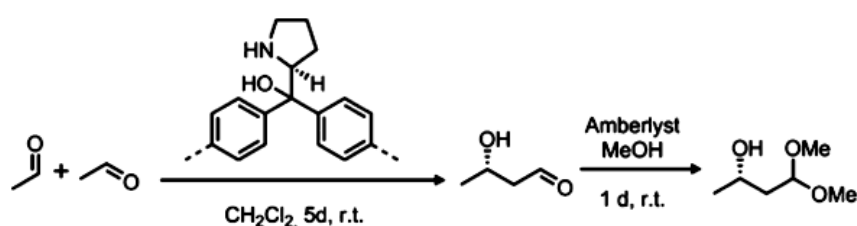
Figure 14. Diagram of potential mechanism for auto tandem catalysis. Reproduced from [54] with permission from Nature Publishing Group.

The chiral MOF, (*R,R*)-salen($\text{Co}(\text{III})$)@IRMOF-3-AM (**13**), was explored as a heterogeneous asymmetric catalyst in the one-pot synthesis of optically active cyclic carbonates from racemic epoxides. The reactions were studied with various epoxides, but the conversion, as well as the enantioselectivity, was reported to be quite low. In the case of styrene oxide, only 8% conversion and less than 1% ee were obtained, which implied that the bulky substituent reduced the rate of diffusion over the catalyst and thereby decreased the catalytic activity [71].

3.1.5. Aldol Condensation

In 2015, Bonnefoy et al. [70] scrutinized the asymmetric aldol condensation reaction between acetone and 4-nitrobenzaldehyde by employing peptide-based chiral MOFs as catalysts. The authors specified that an Al-MIL-101-NH-Gly-Pro (**11aa**) loading with 15 mol% of proline afforded an aldol product of 26% yield with 25% ee, and, likewise, Al-MIL-101-NH-Pro (**11ab**) showed an ee of 18%; whereas 100 mol% of proline moieties in Al-MIL-101-NH-Gly-Pro (**11aa**) increased the yield of product to 80%, but no significant change in enantioselectivity (only 27% ee) was observed.

Fröba and associates [47] synthesized a series of UHM-25 MOFs by introducing chiral amino acid substituents in diisophthalate linkers. Out of these synthesized chiral MOFs, the asymmetric catalytic activity of UHM-25-Pro (**34**) on aldol condensation was examined, over which the self-directed aldol condensation of acetaldehyde and the subsequent conversion of 3-hydroxybutanal to 1,1-Dimethoxy-3-hydroxybutane was scrutinized (Scheme 6). The yield obtained over both steps was 45% with the (*R*)-enantiomer as the major product, and the enantiomeric ratio of the products was 70:30.



Scheme 6. Asymmetric aldol condensation and formation of hemiacetal product catalyzed by UHM-25-Pro. Reproduced from [47] with permission from the American Chemical Society.

3.1.6. Imine Reduction

Recently, Zhang and associates [99] designed a chiral MOF, CMIL-101 (**35**), by grafting chiral pyridyl-modified *N*-formyl-*L*-proline derivatives with MIL-101(Cr), which were further explored for the reduction of ketimine derivatives. The yield of the reaction was good when the reaction was performed at room temperature, and the ee was moderate (only 37%) but higher compared to the corresponding homogeneous catalyst.

3.2. Enantioselective Separation

The enantioselective separation of analytes is an alternative significant field of application for homochiral MOFs. Discovery of chiral adsorbents leads to the development of the rapid separation of individual enantiomers in a cost-effective manner. The method is especially in demand in pharmaceutical, agrochemical, and biomedical research for the enantiopure separation of numerous drugs, as the enantiomers always possess different physiological and pharmacological activities [100]. Homochiral MOFs can be easily designed with chiral channels which are accessible to the analytes along with the ability to change the size and shape of the MOF pores to hold compounds with precise dimensions and assist in separating the isomers. This part of the review describes recent examples of enantiopure separation of racemates by applying chiral MOFs as a stationary phase for high-performance liquid chromatography (HPLC) and high-resolution gas chromatography (GC).

3.2.1. High-performance Liquid Chromatographic (HPLC) Analysis

Nuzhdin et al. [101] were the first to report the liquid chromatographic separation of racemic mixtures of chiral alkyl aryl sulfoxides by employing the chiral MOF, $[\text{Zn}_2(\text{bdc})(L\text{-lac})(\text{dmf})]\cdot\text{DMF}$ (**36**), as a stationary phase. Cui group [102] presented two thermally stable and homochiral 1,10-biphenol-based MOFs having chiral dihydroxyl and dimethoxy groups, respectively. An MOF containing chiral dihydroxyl auxiliaries was employed as a chiral stationary phase of HPLC for the enantioseparation of racemic amines. Parallel to these works, numerous other chiral MOFs, such as $[\text{Cu}_2(d\text{-Cam})_2(4,4'\text{-bpy})]$

(37), $[\text{ZnL}^{18}\text{Br}]\cdot\text{H}_2\text{O}$ (38) ($\text{L}^{18}\cdot\text{HBr} = N\text{-}(4\text{-Pyridylmethyl})\text{-L-leucine}\cdot\text{HBr}$), $[\text{Co}_2(\text{D-cam})_2(\text{TMDPy})]$ (39) ($\text{D-cam} = D\text{-camphorates}$; $\text{TMDPy} = 4,4'\text{-trimethylenedipyridine}$), DUT-32-NHProBoc (40), and $[\text{ZnL}^{19}]_2(\text{NMF})_2\cdot\text{NMF}$ (41) ($\text{L}^{19} = (R)\text{-}2,2'\text{-dihydroxy-}1,1'\text{-binaphthalene-}6,6'\text{-dicarboxylic acid}$; $\text{NMF} = N\text{-methylformamide}$) were synthesized and used for the enantioselective separation of various racemates [33,103–106]. Some of the currently published chiral MOFs, with their remarkable abilities for the separation of the chiral compounds, are discussed below.

In 2016, Yuan and associates [107] designed a homochiral MOF, $[\text{Cd}_2(d\text{-cam})_3]\cdot 2\text{Hdma}\cdot 4\text{dma}$ (42), and applied it as a novel chiral stationary phase in HPLC. Nine racemates, including 1-(1-naphthyl) ethanol, 1-(4-chlorophenyl) ethanol, 1-(9-anthryl)-2,2,2-trifluoroethanol, 1,1'-bi-2-naphthol, benzoin, hydrobenzoin, trans-stilbene oxide, praziquantel, and warfarin sodium, were well-separated on the Cd-MOF column and the highest resolution value obtained was for 1-(1-naphthyl) ethanol ($R_S = 4.55$). The same group [108] recently synthesized six amino-acid-based chiral MOFs, $[\text{Zn}(\text{L-tyr})_n(\text{L-tyrZn})]$ (43a), $[\text{Zn}_4(\text{btc})_2(\text{Hbtc})(\text{L-His})_2(\text{H}_2\text{O})_4]\cdot 1.5\text{H}_2\text{O}$ (43b), $[\text{Zn}_2(\text{Ltrp})_2(\text{bpe})_2(\text{H}_2\text{O})_2](\text{NO}_3)_2\cdot 2\text{H}_2\text{O}$ (43c), $[\text{Co}_2(\text{L-Trp})(\text{INT})_2(\text{H}_2\text{O})_2(\text{ClO}_4)]$ (43d), $[\text{Co}_2(\text{sdba})(\text{L-Trp})_2]$ (43e), and $[\text{Co}(\text{L-Glu})(\text{H}_2\text{O})\cdot\text{H}_2\text{O}]$ (43f). Employing these MOFs as a chiral stationary phase in HPLC, several chiral compounds were well-separated in their enantiopure form. Hartlieb et al. [109] reported a CD-MOF (44) built from alkali metal salts and γ -cyclodextrin ($\gamma\text{-CD}$), which has 40 stereo genic centers. The chirality of $\gamma\text{-CD}$ was induced throughout the structure of CD-MOF (44) and assisted the framework to accomplish the separation of a wide variety of compounds, including alkyl-, vinyl-, and haloaromatics, saturated and unsaturated alicyclic compounds, and chiral compounds, such as limonene and 1-phenylethanol. In the case of the structural isomers of pinene and terpinine, it was observed that the isomer with the exocyclic double bond can be gripped by the CD-MOF for a longer time compared to another isomer possessing an endocyclic double bond. In the case of the separation of haloaromatics, molecular simulations established that both the size of the substituted halogen and the strength of the noncovalent bonding interactions between the analyte and the CD-MOF affect the separation process. Cui and co-workers [110] constructed two novel chiral porous MOFs, $[\text{M}_3\text{L}_2^{20}(\text{BDC})_3]\cdot 3\text{H}_2\text{O}$ [$\text{M} = \text{Zn}$ (45a) and Cd (45b)], from a dipyrindyl-functionalized DHIP ligand ($\text{L}^{20} = 2,3\text{-dihydroimidazo}[1,2\text{-a}]$ pyridine (DHIP)). The Zn-DHIP MOF (45a) showed moderate enantioseparation ability towards the racemic sulfoxides because the N atoms of the imidazole moieties, which are the potential bonding sites, are coordinated to the Zn ion, leading to inefficient interactions between chiral host-guest moieties (Figure 15). Although the Cd-DHIP MOF (45b) showed almost no enantioselective adsorption ability under identical conditions due to the small hole size of the interpenetrating network of the Cd-DHIP MOF (45b), it was noted that electron-donating substituents attached to the aromatic rings of aromatic sulfoxides afforded a higher ee compared to the electron-withdrawing substituents present in the rings, and the highest ee of 46.8% was obtained in case of methyl phenyl sulfoxide.



Figure 15. Enantioseparation of racemic sulfoxides by a Zn-DHIP MOF (45a). Reproduced from [110] with permission from the American Chemical Society.

Hailili et al. [111] studied the enantioselective separation of the chiral compounds (\pm)-ibuprofen and (\pm)-1-phenyl-1,2-ethanediol by the chiral MOF $(\text{Me}_2\text{NH}_2)_2[\text{Mn}_4\text{O}(\text{D-cam})_4]\cdot 5\text{H}_2\text{O}$ (**46**), which acted as a stationary phase in HPLC. A hexane-isopropyl alcohol (96:4, v/v) system was used as a mobile phase, which afforded a prominent baseline resolution for the separation of both pairs of the compounds with high resolution. In case of (\pm)-ibuprofen, 80% valley separation with a good selectivity factor ($\alpha = 6.48$) and resolution ($R_s = 2.02$) was accomplished within only 12 min. The authors stated that the calculated van der Waals energy for adsorbed (+)- and (-)-ibuprofen is -16.5 and -20.1 kcal mol $^{-1}$, respectively, which indicates a stronger interaction with the chiral MOF resulting in a long retention time of (-)-ibuprofen (Figure 16).

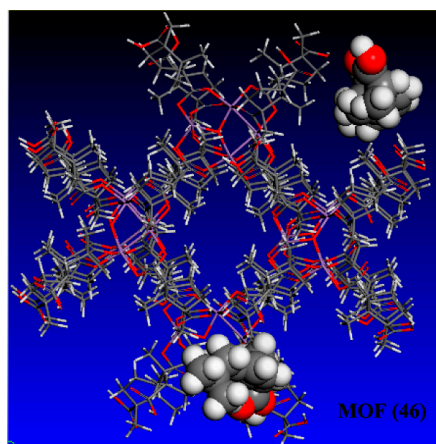


Figure 16. Possible interaction of the (-)-ibuprofen isomer and MOF (**46**) viewed along the c-axis direction. Reproduced from [111] with permission from the American Chemical Society.

Martí-Gastaldo and co-workers [112] recently designed a chiral Cu(II) 3D MOF, $[\text{Cu}(\text{GHG})]$ (**47**), based on the tripeptide Gly-*L*-His-Gly (GHG) for the enantioselective separation of the chiral polar drugs metamphetamine and ephedrine. More than 50% of the (+)-ephedrine enantiomer was isolated when MOF (**47**) was used as a chiral solid phase extraction holder (Figure 17).

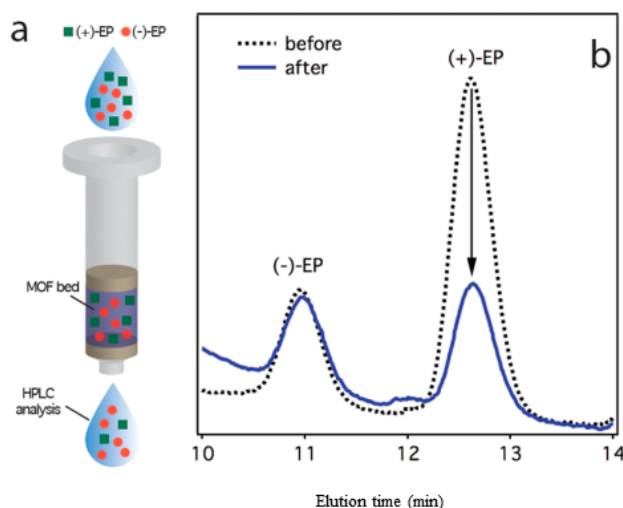


Figure 17. (a) Solid phase extraction separation of ephedrine by using MOF (**47**) as a chiral bed. (b) HPLC chromatograms of ephedrine racemate before (dashed line) and after (solid line) passing through the MOF bed. Reproduced from [112] with permission from the American Chemical Society.

3.2.2. Gas Chromatographic (GC) Analysis

The selection of chromatographic methods is mainly dependent on the properties of the chiral molecules. GC analysis is primarily done for those samples which are thermally stable and volatile. Good resolution, sensitivity, reproducibility, good efficiency, fast analysis, and no need of liquid mobile phases are some of the benefits of GC analysis compared to other chromatographic methods. In 2011, Xie et al. [113] first reported the use of the chiral MOF [Cu(sala)₂(H₂O)] (48) (H₂sala = *N*-(2-hydroxybenzyl)-*L*-alanine) in GC as a chiral stationary phase for the separation of a large number of chiral compounds in their enantiopure forms. Later, the same group designed two new chiral MOFs for upgraded GC separations of enantiomers by combining peramylated β -cyclodextrin with the MOFs [Co(*d*Cam)_{1/2}(bdc)_{1/2}(tmdpy)] (49) and [InH(*d*-C₁₀H₁₄O₄)₂] (50) [114,115]. Numerous other chiral MOFs [116–118] have been designed and successfully reported for the separation of racemates via GC analysis, such as [Zn₂(*D*-Cam)₂(4,4'-bpy)] (51), [Cd(LTP)₂] (52) (LTP = *L*(-)-thiazolidine-4-carboxylic acid), and [Ni(pybz)₂] (53) (pybz = 4-(4-pyridyl)benzoate).

In 2016, Zhang and co-workers [119] constructed a homochiral MOF [Cu^I₂Cu^{II}(L²¹)₂(CN)(H₂O)](NO₃)·DMF (54) (L²¹ = 5-eatz = (1*S*)-1-(5-tetrazolyl) ethylamine) with rare ligand-unsupported Cu-Cu interactions. The synthesized MOF was applied in the enantioselective separation of various racemic alcohols and it was found that the MOF (54) can separate only aromatic alcohols rather than aliphatic alcohols. Two reasons for this unusual behavior of the MOF (54) were stated by the authors: firstly, the entry of large molecules was quite impossible through the 1D narrow network. Thus, enantioselective separation was likely to occur on the chiral surface of the MOF, where aromatic alcohols could be separated more easily compared to aliphatic alcohols. Secondly, enantiomeric separation of aromatic alcohols was possible due to the existence of three types of interaction, i.e., the π - π interactions between the surface of the MOF and aromatic alcohols, and H-bonding and stereochemical interactions with the chiral L²⁰ ligands on the MOF surface. In the case of aliphatic alcohols, only H-bonding interactions happened, which led to no enantioselective separation. Figure 18 shows the possible mechanism of enantioselective separation by the chiral MOF.

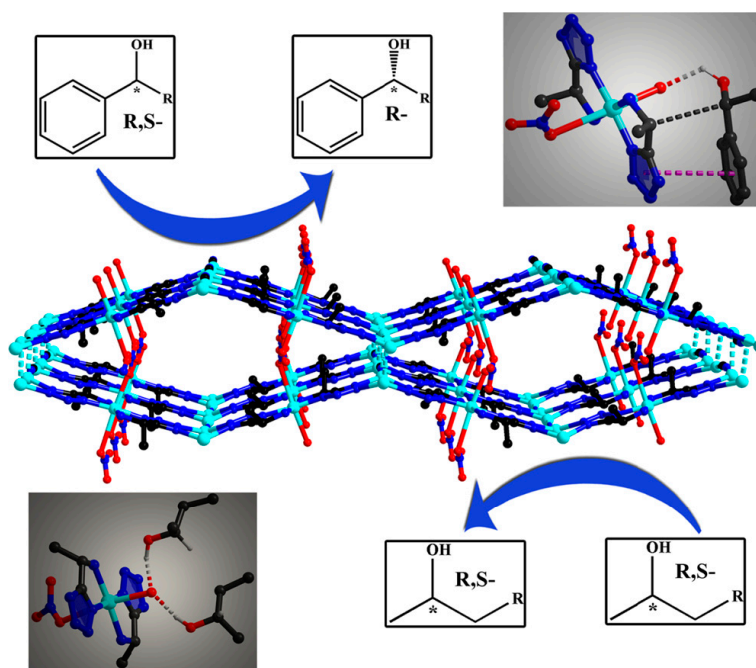


Figure 18. Possible interactions between the chiral framework and chiral alcohols. Reproduced from [119] with permission from the American Chemical Society.

Recently, Lang et al. [120] reported a homochiral MOF, Co-*L*-GG (55) (*L*-GG = dipeptide H-Gly-*L*-Glu), as a stationary phase for the enantiomeric separation of racemates. Around 30 racemates, including halohydrocarbons, ketones, esters, ethers, organic acids, epoxy alkanes, sulfoxides, alcohols, and isomers, were studied and it was demonstrated that the column has significant ability towards chiral recognition and the selective separation of enantiomers.

4. Conclusions and Prospects

This review summarizes the present progress of the synthesis of chiral MOFs and their applications as catalysts in asymmetric reactions and chiral stationary phase in the enantioselective separation of chiral molecules. Although the process is expensive, the synthesis of chiral MOFs has greatly expanded from pre-synthesized chiral ligands. Other methods for the synthesis of chiral MOFs are still in progress. The applications of chiral MOFs as heterogeneous catalysts in asymmetric reactions have proved themselves to be outstanding catalysts by affording greater yields and enantioselectivities of reactions compared to those of the homogeneous control catalysts. However, these MOF catalysts are facing trouble in the case of sterically hindered reagents, which have been found to be futile for proceeding with asymmetric reactions with good enantioselectivities. It was observed that numerous organic transformations were done by post-metallated MOFs or MOFs prepared from salen ligands. Chromatographic separation with chiral MOFs has expanded very rapidly in the last 10 years and many more suitable chiral MOFs have been designed for the separation of various organic racemates. Some of the promising results were elaborately discussed in this review to present the advancement of the field. Besides the chiral MOFs, other alternative frameworks, such as covalent organic frameworks (COFs) [121,122] and defect porous organic frameworks (dPOFs) [123], are newly emerging fields in the chiral world. The present review hopefully benefits researchers to design chiral MOFs by various methods and serves as a driving force for them to explore applications of the synthesized chiral MOFs in various new fields.

Acknowledgments: We thank the One Thousand Young Talents Program under the Recruitment Program of Global Experts, the National Natural Science Foundation of China (NSFC) (21233009), the Strategic Priority Research Program of the Chinese Academy of Sciences (CAS) (XDB20010200), and the 973 Program (2014CB845603) for financial support.

Conflicts of Interest: The authors declare no conflict of interest.

References

1. Furukawa, H.; Cordova, K.E.; O’Keeffe, M.; Yaghi, O.M. The Chemistry and Applications of Metal–Organic Frameworks. *Science* **2013**, *341*, 1230444. [[CrossRef](#)] [[PubMed](#)]
2. Kim, C.R.; Uemura, T.; Kitagawa, S. Inorganic nanoparticles in porous coordination polymers. *Chem. Soc. Rev.* **2016**, *45*, 3828–3845. [[CrossRef](#)] [[PubMed](#)]
3. Zhao, D.; Timmons, D.J.; Yuan, D.; Zhou, H.-C. Tuning the Topology and Functionality of Metal–Organic Frameworks by Ligand Design. *Acc. Chem. Res.* **2011**, *44*, 123–133. [[CrossRef](#)] [[PubMed](#)]
4. Li, B.; Wen, H.-M.; Cui, Y.; Zhou, W.; Qian, G.; Chen, B. Emerging Multifunctional Metal–Organic Framework Materials. *Adv. Mater.* **2016**, *28*, 8819–8860. [[CrossRef](#)] [[PubMed](#)]
5. Zhu, Q.-L.; Xu, Q. Metal–organic framework composites. *Chem. Soc. Rev.* **2014**, *43*, 5468–5512. [[CrossRef](#)] [[PubMed](#)]
6. Zhu, Q.-L.; Li, J.; Xu, Q. Immobilizing Metal Nanoparticles to Metal–Organic Frameworks with Size and Location Control for Optimizing Catalytic Performance. *J. Am. Chem. Soc.* **2013**, *135*, 10210–10213. [[CrossRef](#)] [[PubMed](#)]
7. Yang, Q.; Xu, Q.; Jiang, H.-L. Metal–Organic Frameworks Meet Metal Nanoparticles: Synergistic Effect for Enhanced Catalysis. *Chem. Soc. Rev.* **2017**, *46*, 4774–4808. [[CrossRef](#)] [[PubMed](#)]
8. Li, B.; Wen, H.-M.; Zhou, W.; Xu, J.Q.; Chen, B. Porous Metal–Organic Frameworks: Promising Materials for Methane Storage. *Chem* **2016**, *1*, 557–580. [[CrossRef](#)]

9. Suh, M.P.; Park, H.J.; Prasad, T.K.; Lim, D.-W. Hydrogen Storage in Metal–Organic Frameworks. *Chem. Rev.* **2012**, *112*, 782–835. [[CrossRef](#)] [[PubMed](#)]
10. Li, J.-R.; Scully, J.; Zhou, H.-C. Metal–Organic Frameworks for Separations. *Chem. Rev.* **2012**, *112*, 869–932. [[CrossRef](#)] [[PubMed](#)]
11. Van de Voorde, B.; Bueken, B.; Denayer, J.; De Vos, D. Adsorptive separation on metal–organic frameworks in the liquid phase. *Chem. Soc. Rev.* **2014**, *43*, 5766–5788. [[CrossRef](#)] [[PubMed](#)]
12. Li, X.; Chang, C.; Wang, X.; Bai, Y.; Liu, H. Applications of homochiral metal-organic frameworks in enantioselective adsorption and chromatography separation. *Electrophoresis* **2014**, *35*, 2733–2743. [[CrossRef](#)] [[PubMed](#)]
13. Kreno, L.E.; Leong, K.; Farha, O.K.; Allendorf, M.; Van Duyne, R.P.; Hupp, J.T. Metal–Organic Framework Materials as Chemical Sensors. *Chem. Rev.* **2012**, *112*, 1105–1125. [[CrossRef](#)] [[PubMed](#)]
14. Cao, K.-L.; Xia, Y.; Wang, G.-X.; Feng, Y.-L. A robust luminescent Ba (II) metal–organic framework based on pyridine carboxylate ligand for sensing of small molecules. *Inorg. Chem. Commun.* **2015**, *53*, 42–45. [[CrossRef](#)]
15. Zhao, X.-L.; Tian, D.; Gao, Q.; Sun, H.-W.; Xu, J.; Bu, X.-H. The international journal for high quality, original research in inorganic and organometallic chemistry. *Dalton Trans.* **2016**, *45*, 845.
16. Wanderley, M.M.; Wang, C.; Wu, C.-D.; Lin, W. A Chiral Porous Metal-Organic Framework for Highly Sensitive and Enantioselective Fluorescence Sensing of Amino Alcohols. *J. Am. Chem. Soc.* **2012**, *134*, 9050–9053. [[CrossRef](#)] [[PubMed](#)]
17. Qiu, S.; Xue, M.; Zhu, G. Metal–organic framework membranes: From synthesis to separation application. *Chem. Soc. Rev.* **2014**, *43*, 6116–6140. [[CrossRef](#)] [[PubMed](#)]
18. Duerinck, T.; Denayer, J.F.M. Metal-organic frameworks as stationary phases for chiral chromatographic and membrane separations. *Chem. Eng. Sci.* **2015**, *124*, 179–187. [[CrossRef](#)]
19. Horcajada, P.; Gref, R.; Baati, T.; Allan, P.K.; Maurin, G.; Couvreur, P.; Férey, G.; Morris, R.E.; Serre, C. Metal–Organic Frameworks in Biomedicine. *Chem. Rev.* **2012**, *112*, 1232–1268. [[CrossRef](#)] [[PubMed](#)]
20. Sha, J.-Q.; Zhong, X.-H.; Wu, L.-H.; Liu, G.-D.; Sheng, N. Nontoxic and renewable metal–organic framework based on $[\alpha]$ -cyclodextrin with efficient drug delivery. *RSC Adv.* **2016**, *6*, 82977–82983. [[CrossRef](#)]
21. Liu, M.; Zhang, L.; Wang, T. Supramolecular Chirality in Self-Assembled Systems. *Chem. Rev.* **2015**, *115*, 7304–7397. [[CrossRef](#)] [[PubMed](#)]
22. Kumar, J.; Thomas, K.G.; Liz-Marzan, L.M. Nanoscale chirality in metal and semiconductor nanoparticles. *Chem. Commun.* **2016**, *52*, 12555–12569. [[CrossRef](#)] [[PubMed](#)]
23. Zhang, Z.-M.; Duan, X.; Yao, S.; Wang, Z.; Lin, Z.; Li, Y.-G.; Long, L.-S.; Wang, E.-B.; Lin, W. Cation-mediated optical resolution and anticancer activity of chiral polyoxometalates built from entirely achiral building blocks. *Chem. Sci.* **2016**, *7*, 4220–4229. [[CrossRef](#)]
24. Burneo Saavedra, I.P. Metal-Organic Frameworks Made of Amino Acids and Adenine: Chirality and Hydrochromism. Available online: <http://hdl.handle.net/10803/457357> (accessed on 18 March 2018).
25. Yoon, M.; Srirambalaji, R.; Kim, K. Homochiral Metal–Organic Frameworks for Asymmetric Heterogeneous Catalysis. *Chem. Rev.* **2012**, *112*, 1196–1231. [[CrossRef](#)] [[PubMed](#)]
26. Song, F.; Wang, C.; Lin, W. A chiral metal–organic framework for sequential asymmetric catalysis. *Chem. Commun.* **2011**, *47*, 8256–8258. [[CrossRef](#)] [[PubMed](#)]
27. Wang, C.; Zheng, M.; Lin, W. Asymmetric Catalysis with Chiral Porous Metal-Organic Frameworks: Critical Issues. *J. Phys. Chem. Lett.* **2011**, *2*, 1701–1709. [[CrossRef](#)]
28. Leus, K.; Liu, Y.Y.; Voort, P.V.D. Metal–Organic Frameworks as Selective or Chiral Oxidation Catalysts. *Catal. Rev. Sci. Eng.* **2014**, *56*, 1–56. [[CrossRef](#)]
29. Liu, S.; Shinde, S.; Pan, J.; Ma, Y.; Yan, Y.; Pan, G. Interface-induced growth of boronate-based metal-organic framework membrane on porous carbon substrate for aqueous phase molecular recognition. *Chem. Eng. J.* **2017**, *324*, 216–227. [[CrossRef](#)]
30. Mendiratta, S.; Lee, C.-H.; Lee, S.-Y.; Kao, Y.-C.; Chang, B.-C.; Lo, Y.-H.; Lu, K.-L. Structural Characteristics and Non-Linear Optical Behaviour of a 2-Hydroxynicotinate-Containing Zinc-Based Metal–Organic Framework. *Molecules* **2015**, *20*, 8941–8951. [[CrossRef](#)] [[PubMed](#)]
31. Li, H.-Y.; Xu, H.; Zang, S.-Q.; Mak, T.C.W. A viologen-functionalized chiral Eu-MOF as a platform for multifunctional switchable material. *Chem. Commun.* **2016**, *52*, 525–528. [[CrossRef](#)] [[PubMed](#)]

32. Sun, Y.-Q.; Liu, Q.; Liu, L.-H.; Ding, L.; Chen, Y.-P. Two 3D nonlinear optical and luminescent lanthanide–organic frameworks with multidirectional helical intersecting channels. *New J. Chem.* **2017**, *41*, 6736–6741. [[CrossRef](#)]
33. Kong, J.; Zhang, M.; Duan, A.-H.; Zhang, J.-H.; Yang, R.; Yuan, L.-M. Homochiral metal–organic framework used as a stationary phase for high-performance liquid chromatography. *J. Sep. Sci.* **2015**, *38*, 556–561. [[CrossRef](#)] [[PubMed](#)]
34. Li, P.; He, Y.; Guang, J.; Weng, L.; Zhao, J.C.-G.; Xiang, S.; Chen, B. A Homochiral Microporous Hydrogen-Bonded Organic Framework for Highly Enantioselective Separation of Secondary Alcohols. *J. Am. Chem. Soc.* **2014**, *136*, 547–549. [[CrossRef](#)] [[PubMed](#)]
35. Okamoto, Y.; Ikai, T. Chiral HPLC for efficient resolution of enantiomers. *Chem. Soc. Rev.* **2008**, *37*, 2593–2608. [[CrossRef](#)] [[PubMed](#)]
36. Cavazzini, A.; Pasti, L.; Massi, A.; Marchetti, N.; Dondi, F. Recent applications in chiral high performance liquid chromatography: A review. *Anal. Chim. Acta* **2011**, *706*, 205–222. [[CrossRef](#)] [[PubMed](#)]
37. Chang, C.; Wang, X.; Bai, Y.; Liu, H. Applications of nanomaterials in enantioselective separation and related techniques. *Trends Anal. Chem.* **2012**, *39*, 195–206. [[CrossRef](#)]
38. Lin, W. Asymmetric Catalysis with Chiral Porous Metal–Organic Frameworks. *Top. Catal.* **2010**, *53*, 869–875. [[CrossRef](#)]
39. Ma, L.; Abney, C.; Lin, W. Enantioselective catalysis with homochiral metal–organic frameworks. *Chem. Soc. Rev.* **2009**, *38*, 1248–1256. [[CrossRef](#)] [[PubMed](#)]
40. Gu, Z.-G.; Zhan, C.; Zhang, J.; Bu, X. Chiral chemistry of metal–camphorate frameworks. *Chem. Soc. Rev.* **2016**, *45*, 3122–3144. [[CrossRef](#)] [[PubMed](#)]
41. Nickerl, G.; Henschel, A.; Grüner, R.; Gedrich, K.; Kaskel, S. Chiral Metal–Organic Frameworks and Their Application in Asymmetric Catalysis and Stereoselective Separation. *Chem. Ing. Tech.* **2011**, *83*, 90–103. [[CrossRef](#)]
42. Bisht, K.K.; Parmar, B.; Rachuri, Y.; Kathalikattil, A.C.; Suresh, E. Progress in the synthetic and functional aspects of chiral metal–organic frameworks. *CrystEngComm* **2015**, *17*, 5341–5356. [[CrossRef](#)]
43. Han, Z.; Shi, W.; Cheng, P. Synthetic strategies for chiral metal–organic frameworks. *Chin. Chem. Lett.* **2017**. [[CrossRef](#)]
44. Seo, J.S.; Whang, D.; Lee, H.; Jun, S.I.; Oh, J.; Jeon, Y.J.; Kim, K. A homochiral metal–organic porous material for enantioselective separation and catalysis. *Nature* **2000**, *404*, 982. [[CrossRef](#)] [[PubMed](#)]
45. Ingleson, M.J.; Barrio, J.P.; Bacsá, J.; Dickinson, C.; Park, H.; Rosseinsky, M.J. Generation of a solid Bronsted acid site in a chiral framework. *Chem. Commun.* **2008**, 1287–1289. [[CrossRef](#)] [[PubMed](#)]
46. Rebilly, J.-N.; Bacsá, J.; Rosseinsky, M.J. 1 D Tubular and 2 D Metal–Organic Frameworks Based on a Flexible Amino Acid Derived Organic Spacer. *Chem. Asian J.* **2009**, *4*, 892–903. [[CrossRef](#)] [[PubMed](#)]
47. Sartor, M.; Stein, T.; Hoffmann, F.; Fröba, M. A New Set of Isoreticular, Homochiral Metal–Organic Frameworks with ucp Topology. *Chem. Mater.* **2016**, *28*, 519–528. [[CrossRef](#)]
48. Zhu, Q.; Sheng, T.; Fu, R.; Tan, C.; Hu, S.; Wu, X. Two luminescent enantiomorphic 3D metal–organic frameworks with 3D homochiral double helices. *Chem. Commun.* **2010**, *46*, 9001–9003. [[CrossRef](#)] [[PubMed](#)]
49. Hu, G.; Zhang, H.; Miao, H.; Wang, J.; Xu, Y. Synthesis, structures and properties of two new chiral rare earth–organic frameworks constructed by l/d-tartaric acid. *J. Solid State Chem.* **2015**, *229*, 208–212. [[CrossRef](#)]
50. Ren, W.X.; Jian, L.Z.; Wei, G.; Yan, L.; Zhan, L.B.; Yong, C. A Novel TADDOL-based Chiral Metal–organic Framework: Synthesis, Structure and Photoluminescence Study. *Chin. J. Struct. Chem.* **2016**, *35*, 1399–1405.
51. Evans, O.R.; Ngo, H.L.; Lin, W. Chiral Porous Solids Based on Lamellar Lanthanide Phosphonates. *J. Am. Chem. Soc.* **2001**, *123*, 10395–10396. [[CrossRef](#)] [[PubMed](#)]
52. Ma, L.; Falkowski, J.M.; Abney, C.; Lin, W. A series of isoreticular chiral metal–organic frameworks as a tunable platform for asymmetric catalysis. *Nat. Chem.* **2010**, *2*, 838. [[CrossRef](#)] [[PubMed](#)]
53. Wu, C.D.; Hu, A.; Zhang, L.; Lin, W. A Homochiral Porous Metal–Organic Framework for Highly Enantioselective Heterogeneous Asymmetric Catalysis. *J. Am. Chem. Soc.* **2005**, *127*, 8940–8941. [[CrossRef](#)] [[PubMed](#)]
54. Han, Q.; Qi, B.; Ren, W.; He, C.; Niu, J.; Duan, C. Polyoxometalate-based homochiral metal–organic frameworks for tandem asymmetric transformation of cyclic carbonates from olefins. *Nat. Commun.* **2015**, *6*, 10007. [[CrossRef](#)] [[PubMed](#)]

55. Kuang, X.; Ye, S.; Li, X.; Ma, Y.; Zhang, C.; Tang, B. A new type of surface-enhanced Raman scattering sensor for the enantioselective recognition of d/l-cysteine and d/l-asparagine based on a helically arranged Ag NPs@homochiral MOF. *Chem. Commun.* **2016**, *52*, 5432–5435. [[CrossRef](#)] [[PubMed](#)]
56. Li, M.-Y.; Wang, F.; Gu, Z.-G.; Zhang, J. Synthesis of homochiral zeolitic metal–organic frameworks with amino acid and tetrazolates for chiral recognition. *RSC Adv.* **2017**, *7*, 4872–4875. [[CrossRef](#)]
57. Gupta, A.K.; De, D.; Katoch, R.; Garg, A.; Bharadwaj, P.K. Synthesis of a NbO Type Homochiral Cu(II) Metal–Organic Framework: Ferroelectric Behavior and Heterogeneous Catalysis of Three-Component Coupling and Pechmann Reactions. *Inorg. Chem.* **2017**, *56*, 4697–4705. [[CrossRef](#)] [[PubMed](#)]
58. Yang, J.; Trickett, C.A.; Alahmadi, S.B.; Alshammari, A.S.; Yaghi, O.M. Calcium L-Lactate Frameworks as Naturally Degradable Carriers for Pesticides. *J. Am. Chem. Soc.* **2017**, *139*, 8118–8121. [[CrossRef](#)] [[PubMed](#)]
59. Robin, J.; Audebrand, N.; Poriol, C.; Canivet, J.; Calvez, G.; Roisnel, T.; Dorcet, V.; Roussel, P. A series of chiral metal–organic frameworks based on fluorene di- and tetra-carboxylates: Syntheses, crystal structures and luminescence properties. *CrystEngComm* **2017**, *19*, 2042–2056. [[CrossRef](#)]
60. Kutzscher, C.; Janssen-Muller, D.; Notzon, A.; Stoeck, U.; Bon, V.; Senkovska, I.; Kaskel, S.; Glorius, F. Synthesis of the homochiral metal–organic framework DUT-129 based on a chiral dicarboxylate linker with 6 stereocenters. *CrystEngComm* **2017**, *19*, 2494–2499. [[CrossRef](#)]
61. Cho, S.-H.; Ma, B.; Nguyen, S.T.; Hupp, J.T.; Albrecht-Schmitt, T.E. A metal–organic framework material that functions as an enantioselective catalyst for olefin epoxidation. *Chem. Commun.* **2006**, 2563–2565. [[CrossRef](#)] [[PubMed](#)]
62. Liu, Y.; Li, Z.; Yuan, G.; Xia, Q.; Yuan, C.; Cui, Y. Chiral Cu(salen)-Based Metal–Organic Framework for Heterogeneously Catalyzed Aziridination and Amination of Olefins. *Inorg. Chem.* **2016**, *55*, 12500–12503. [[CrossRef](#)] [[PubMed](#)]
63. Fan, Y.; Li, J.; Ren, Y.; Jiang, H. A Ni(salen)-Based Metal–Organic Framework: Synthesis, Structure, and Catalytic Performance for CO₂ Cycloaddition with Epoxides. *Eur. J. Inorg. Chem.* **2017**, 4982–4989. [[CrossRef](#)]
64. Li, J.; Ren, Y.; Qi, C.; Jiang, H. A chiral salen-based MOF catalytic material with high thermal, aqueous and chemical stabilities. *Dalton Trans.* **2017**, *46*, 7821–7832. [[CrossRef](#)] [[PubMed](#)]
65. Xia, Q.; Li, Z.; Tan, C.; Liu, Y.; Gong, W.; Cui, Y. Multivariate Metal–Organic Frameworks as Multifunctional Heterogeneous Asymmetric Catalysts for Sequential Reactions. *J. Am. Chem. Soc.* **2017**, *139*, 8259–8266. [[CrossRef](#)] [[PubMed](#)]
66. Wang, Z.; Cohen, S.M. Postsynthetic modification of metal–organic frameworks. *Chem. Soc. Rev.* **2009**, *38*, 1315–1329. [[CrossRef](#)] [[PubMed](#)]
67. Wang, Z.; Cohen, S.M. Tandem Modification of Metal–Organic Frameworks by a Postsynthetic Approach. *Angew. Chem. Int. Ed.* **2008**, *47*, 4699–4702. [[CrossRef](#)] [[PubMed](#)]
68. Tanabe, K.K.; Cohen, S.M. Engineering a Metal–Organic Framework Catalyst by Using Postsynthetic Modification. *Angew. Chem. Int. Ed.* **2009**, *48*, 7424–7427. [[CrossRef](#)] [[PubMed](#)]
69. Garibay, S.J.; Wang, Z.; Tanabe, K.K.; Cohen, S.M. Postsynthetic Modification: A Versatile Approach toward Multifunctional Metal–Organic Frameworks. *Inorg. Chem.* **2009**, *48*, 7341–7349. [[CrossRef](#)] [[PubMed](#)]
70. Bonnefoy, J.; Legrand, A.; Quadrelli, E.A.; Canivet, J.; Farrusseng, D. Enantiopure Peptide-Functionalized Metal–Organic Frameworks. *J. Am. Chem. Soc.* **2015**, *137*, 9409–9416. [[CrossRef](#)] [[PubMed](#)]
71. Chen, D.; Luo, R.; Li, M.; Wen, M.; Li, Y.; Chen, C.; Zhang, N. Salen(Co(III)) imprisoned within pores of a metal–organic framework by post-synthetic modification and its asymmetric catalysis for CO₂ fixation at room temperature. *Chem. Commun.* **2017**, *53*, 10930–10933. [[CrossRef](#)] [[PubMed](#)]
72. Hou, X.; Xu, T.; Wang, Y.; Liu, S.; Tong, J.; Liu, B. Superficial Chiral Etching on Achiral Metal–Organic Framework for Enantioselective Sorption. *ACS Appl. Mater. Interfaces* **2017**, *9*, 32264–32269. [[CrossRef](#)] [[PubMed](#)]
73. Ezuhara, T.; Endo, K.; Aoyama, Y. Helical Coordination Polymers from Achiral Components in Crystals. Homochiral Crystallization, Homochiral Helix Winding in the Solid State, and Chirality Control by Seeding. *J. Am. Chem. Soc.* **1999**, *121*, 3279–3283. [[CrossRef](#)]
74. Li, Z.; Du, L.; Zhou, J.; Li, L.; Hu, Y.; Qiao, Y.; Xie, M.; Zhao, Q. A chiral porous cobalt-organic framework based on reinforced sinusoidal-like SBUs involving in situ-generated formate. *New J. Chem.* **2013**, *37*, 2473–2478. [[CrossRef](#)]

75. Durá, G.; Carrión, M.C.; Jalón, F.A.; Rodríguez, A.M.; Manzano, B.R. Self-Assembly of Silver(I) and Ditopic Heteroscorpionate Ligands. Spontaneous Chiral Resolution in Helices and Sequence Isomerism in Coordination Polymers. *Cryst. Growth Des.* **2013**, *13*, 3275–3282. [[CrossRef](#)]
76. Liu, W.; Bao, X.; Mao, L.-L.; Tucek, J.; Zboril, R.; Liu, J.-L.; Guo, F.-S.; Ni, Z.-P.; Tong, M.-L. A chiral spin crossover metal–organic framework. *Chem. Commun.* **2014**, *50*, 4059–4061. [[CrossRef](#)] [[PubMed](#)]
77. Sun, Q.; Cheng, A.-L.; Wang, K.; Yi, X.-C.; Gao, E.-Q. Chiral or achiral: Four isomeric Cd(II) coordination polymers based on phenylenediacylate ligands. *CrystEngComm* **2015**, *17*, 1389–1397. [[CrossRef](#)]
78. Mei, H.-X.; Zhang, T.; Wang, D.-F.; Huang, R.-B.; Zheng, L.-S. A Zn-oxalate helix linked by a water helix: Spontaneous chiral resolution of a Zn helical coordination polymer. *New J. Chem.* **2015**, *39*, 2075–2080. [[CrossRef](#)]
79. Li, X.; Yu, Z.; Li, X.; Guo, X. Solvent-Mediated Transformation from Achiral to Chiral Nickel(II) Metal–Organic Frameworks and Reassembly in Solution. *Chem. Eur. J.* **2015**, *21*, 16593–16600. [[CrossRef](#)] [[PubMed](#)]
80. Verma, A.; De, D.; Tomar, K.; Bharadwaj, P.K. Chiral Cadmium(II) Metal–Organic Framework from an Achiral Ligand by Spontaneous Resolution: An Efficient Heterogeneous Catalyst for the Strecker Reaction of Ketones. *Inorg. Chem.* **2017**, *56*, 13629–13633. [[CrossRef](#)] [[PubMed](#)]
81. Lin, Z.; Slawin, A.M.Z.; Morris, R.E. Chiral Induction in the Ionothermal Synthesis of a 3-D Coordination Polymer. *J. Am. Chem. Soc.* **2007**, *129*, 4880–4881. [[CrossRef](#)] [[PubMed](#)]
82. Morris, R.E.; Bu, X. Induction of chiral porous solids containing only achiral building blocks. *Nat. Chem.* **2010**, *2*, 353. [[CrossRef](#)] [[PubMed](#)]
83. Jing, X.; He, C.; Dong, D.; Yang, L.; Duan, C. Homochiral Crystallization of Metal–Organic Silver Frameworks: Asymmetric [3+2] Cycloaddition of an Azomethine Ylide. *Angew. Chem. Int. Ed.* **2012**, *51*, 10127–10131. [[CrossRef](#)] [[PubMed](#)]
84. Bisht, K.K.; Suresh, E. Spontaneous Resolution to Absolute Chiral Induction: Pseudo-Kagomé Type Homochiral Zn(II)/Co(II) Coordination Polymers with Achiral Precursors. *J. Am. Chem. Soc.* **2013**, *135*, 15690–15693. [[CrossRef](#)] [[PubMed](#)]
85. Zhang, S.-Y.; Li, D.; Guo, D.; Zhang, H.; Shi, W.; Cheng, P.; Wojtas, L.; Zaworotko, M.J. Synthesis of a Chiral Crystal Form of MOF-5, CMOF-5, by Chiral Induction. *J. Am. Chem. Soc.* **2015**, *137*, 15406–15409. [[CrossRef](#)] [[PubMed](#)]
86. Li, Y.; Weng, Z.; Wang, Y.; Chen, L.; Sheng, D.; Liu, Y.; Diwu, J.; Chai, Z.; Albrecht-Schmitt, T.E.; Wang, S. Centrosymmetric and chiral porous thorium organic frameworks exhibiting uncommon thorium coordination environments. *Dalton Trans.* **2015**, *44*, 20867–20873. [[CrossRef](#)] [[PubMed](#)]
87. Song, B.-Q.; Chen, D.-Q.; Ji, Z.; Tang, J.; Wang, X.-L.; Zang, H.-Y.; Su, Z.-M. Control of bulk homochirality and proton conductivity in isostructural chiral metal–organic frameworks. *Chem. Commun.* **2017**, *53*, 1892–1895. [[CrossRef](#)] [[PubMed](#)]
88. Wu, S.-T.; Cai, Z.-W.; Ye, Q.-Y.; Weng, C.-H.; Huang, X.-H.; Hu, X.-L.; Huang, C.-C.; Zhuang, N.-F. Enantioselective Synthesis of a Chiral Coordination Polymer with Circularly Polarized Visible Laser. *Angew. Chem. Int. Ed.* **2014**, *53*, 12860–12864. [[CrossRef](#)] [[PubMed](#)]
89. Falkowski, J.M.; Sawano, T.; Zhang, T.; Tsun, G.; Chen, Y.; Lockard, J.V.; Lin, W. Privileged Phosphine-Based Metal–Organic Frameworks for Broad-Scope Asymmetric Catalysis. *J. Am. Chem. Soc.* **2014**, *136*, 5213–5216. [[CrossRef](#)] [[PubMed](#)]
90. Sawano, T.; Thacker, N.C.; Lin, Z.; McIsaac, A.R.; Lin, W. Robust, Chiral, and Porous BINAP-Based Metal–Organic Frameworks for Highly Enantioselective Cyclization Reactions. *J. Am. Chem. Soc.* **2015**, *137*, 12241–12248. [[CrossRef](#)] [[PubMed](#)]
91. Sawano, T.; Ji, P.; McIsaac, A.R.; Lin, Z.; Abney, C.W.; Lin, W. The first chiral diene-based metal–organic frameworks for highly enantioselective carbon-carbon bond formation reactions. *Chem. Sci.* **2015**, *6*, 7163–7168. [[CrossRef](#)]
92. Lee, M.; Shin, S.M.; Jeong, N.; Thallapally, P.K. Chiral environment of catalytic sites in the chiral metal–organic frameworks. *Dalton Trans.* **2015**, *44*, 9349–9352. [[CrossRef](#)] [[PubMed](#)]
93. Tanaka, K.; Nagase, S.; Anami, T.; Wierzbicki, M.; Urbanczyk-Lipkowska, Z. Enantioselective Diels-Alder reaction in the confined space of homochiral metal–organic frameworks. *RSC Adv.* **2016**, *6*, 111436–111439. [[CrossRef](#)]
94. Xia, Q.; Liu, Y.; Li, Z.; Gong, W.; Cui, Y. A Cr(salen)-based metal–organic framework as a versatile catalyst for efficient asymmetric transformations. *Chem. Commun.* **2016**, *52*, 13167–13170. [[CrossRef](#)] [[PubMed](#)]

95. Mo, K.; Yang, Y.; Cui, Y. A Homochiral Metal–Organic Framework as an Effective Asymmetric Catalyst for Cyanohydrin Synthesis. *J. Am. Chem. Soc.* **2014**, *136*, 1746–1749. [[CrossRef](#)] [[PubMed](#)]
96. Zhu, C.; Xia, Q.; Chen, X.; Liu, Y.; Du, X.; Cui, Y. Chiral Metal–Organic Framework as a Platform for Cooperative Catalysis in Asymmetric Cyanosilylation of Aldehydes. *ACS Catal.* **2016**, *6*, 7590–7596. [[CrossRef](#)]
97. Li, J.; Ren, Y.; Qi, C.; Jiang, H. The first porphyrin-salen based chiral metal–organic framework for asymmetric cyanosilylation of aldehydes. *Chem. Commun.* **2017**, *53*, 8223–8226. [[CrossRef](#)] [[PubMed](#)]
98. Li, Z.; Liu, Y.; Xia, Q.; Cui, Y. Chiral binary metal–organic frameworks for asymmetric sequential reactions. *Chem. Commun.* **2017**, *53*, 12313–12316. [[CrossRef](#)] [[PubMed](#)]
99. Chen, J.; Chen, X.; Zhang, Z.; Bao, Z.; Xing, H.; Yang, Q.; Ren, Q. MIL-101(Cr) as a synergistic catalyst for the reduction of imines with trichlorosilane. *Mol. Catal.* **2018**, *445*, 163–169. [[CrossRef](#)]
100. Ran, R.; You, L.; Di, B.; Hao, W.; Su, M.; Yan, F.; Huang, L. A novel chiral mesoporous binaphthyl-silicas: Preparation, characterization, and application in HPLC. *J. Sep. Sci.* **2012**, *35*, 1854–1862. [[CrossRef](#)] [[PubMed](#)]
101. Nuzhdin, A.L.; Dybtsev, D.N.; Bryliakov, K.P.; Talsi, E.P.; Fedin, V.P. Enantioselective Chromatographic Resolution and One-Pot Synthesis of Enantiomerically Pure Sulfoxides over a Homochiral Zn–Organic Framework. *J. Am. Chem. Soc.* **2007**, *129*, 12958–12959. [[CrossRef](#)] [[PubMed](#)]
102. Peng, Y.; Gong, T.; Zhang, K.; Lin, X.; Liu, Y.; Jiang, J.; Cui, Y. Engineering chiral porous metal–organic frameworks for enantioselective adsorption and separation. *Nat. Commun.* **2014**, *5*, 4406. [[CrossRef](#)] [[PubMed](#)]
103. Kuang, X.; Ma, Y.; Su, H.; Zhang, J.; Dong, Y.-B.; Tang, B. High-Performance Liquid Chromatographic Enantioseparation of Racemic Drugs Based on Homochiral Metal–Organic Framework. *Anal. Chem.* **2014**, *86*, 1277–1281. [[CrossRef](#)] [[PubMed](#)]
104. Zhang, M.; Zhang, J.-H.; Zhang, Y.; Wang, B.-J.; Xie, S.-M.; Yuan, L.-M. Chromatographic study on the high performance separation ability of a homochiral $[\text{Cu}_2(\text{d-Cam})_2(4,4'\text{-bpy})]_n$ based-column by using racemates and positional isomers as test probes. *J. Chromatogr. A* **2014**, *1325*, 163–170. [[CrossRef](#)] [[PubMed](#)]
105. Kutzscher, C.; Hoffmann, H.C.; Krause, S.; Stoeck, U.; Senkovska, I.; Brunner, E.; Kaskel, S. Proline Functionalization of the Mesoporous Metal–Organic Framework DUT-32. *Inorg. Chem.* **2015**, *54*, 1003–1009. [[CrossRef](#)] [[PubMed](#)]
106. Tanaka, K.; Muraoka, T.; Otubo, Y.; Takahashi, H.; Ohnishi, A. HPLC enantioseparation on a homochiral MOF-silica composite as a novel chiral stationary phase. *RSC Adv.* **2016**, *6*, 21293–21301. [[CrossRef](#)]
107. Zhang, M.; Chen, X.; Zhang, J.; Kong, J.; Yuan, L. A 3D Homochiral MOF $[\text{Cd}_2(\text{d-cam})_3] \cdot 2\text{H}_2\text{O} \cdot 4\text{dma}$ for HPLC Chromatographic Enantioseparation. *Chirality* **2016**, *28*, 340–346. [[CrossRef](#)] [[PubMed](#)]
108. Zhang, J.-H.; Nong, R.-Y.; Xie, S.-M.; Wang, B.-J.; Ai, P.; Yuan, L.-M. Homochiral metal–organic frameworks based on amino acid ligands for HPLC separation of enantiomers. *Electrophoresis* **2017**, *38*, 2513–2520. [[CrossRef](#)] [[PubMed](#)]
109. Hartlieb, K.J.; Holcroft, J.M.; Moghadam, P.Z.; Vermeulen, N.A.; Algaradah, M.M.; Nassar, M.S.; Botros, Y.Y.; Snurr, R.Q.; Stoddart, J.F. CD-MOF: A Versatile Separation Medium. *J. Am. Chem. Soc.* **2016**, *138*, 2292–2301. [[CrossRef](#)] [[PubMed](#)]
110. Zhang, J.; Li, Z.; Gong, W.; Han, X.; Liu, Y.; Cui, Y. Chiral DHIP-Based Metal–Organic Frameworks for Enantioselective Recognition and Separation. *Inorg. Chem.* **2016**, *55*, 7229–7232. [[CrossRef](#)] [[PubMed](#)]
111. Hailili, R.; Wang, L.; Qv, J.; Yao, R.; Zhang, X.-M.; Liu, H. Planar Mn_4O Cluster Homochiral Metal–Organic Framework for HPLC Separation of Pharmaceutically Important (\pm)-Ibuprofen Racemate. *Inorg. Chem.* **2015**, *54*, 3713–3715. [[CrossRef](#)] [[PubMed](#)]
112. Navarro-Sánchez, J.; Argente-García, A.I.; Moliner-Martínez, Y.; Roca-Sanjuán, D.; Antypov, D.; Campíns-Falcó, P.; Rosseinsky, M.J.; Martí-Gastaldo, C. Peptide Metal–Organic Frameworks for Enantioselective Separation of Chiral Drugs. *J. Am. Chem. Soc.* **2017**, *139*, 4294–4297. [[CrossRef](#)] [[PubMed](#)]
113. Xie, S.-M.; Zhang, Z.-J.; Wang, Z.-Y.; Yuan, L.-M. Chiral Metal–Organic Frameworks for High-Resolution Gas Chromatographic Separations. *J. Am. Chem. Soc.* **2011**, *133*, 11892–11895. [[CrossRef](#)] [[PubMed](#)]
114. Liu, H.; Xie, S.-M.; Ai, P.; Zhang, J.-H.; Zhang, M.; Yuan, L.-M. Metal–Organic Framework $\text{Co}(\text{D-Cam})_{1/2}(\text{bcd})_{1/2}(\text{tmdpy})$ for Improved Enantioseparations on a Chiral Cyclodextrin Stationary Phase in Gas Chromatography. *ChemPlusChem* **2014**, *79*, 1103–1108. [[CrossRef](#)]

115. Yang, J.-R.; Xie, S.-M.; Liu, H.; Zhang, J.-H.; Yuan, L.-M. Metal–Organic Framework $\text{InH}(\text{d-C}_{10}\text{H}_{14}\text{O}_4)_2$ for Improved Enantioseparations on a Chiral Cyclodextrin Stationary Phase in GC. *Chromatographia* **2015**, *78*, 557–564. [[CrossRef](#)]
116. Xue, X.; Zhang, M.; Xie, S.; Yuan, L. Homochiral metal–organic framework $[\text{Zn}_2(\text{d-Cam})_2(4,4'\text{-bpy})]_n$ for high-resolution gas chromatographic separations. *Acta Chromatogr.* **2015**, *27*, 15–26. [[CrossRef](#)]
117. Yang, J.-R.; Xie, S.-M.; Zhang, J.-H.; Chen, L.; Nong, R.-Y.; Yuan, L.-M. Metal–Organic Framework $[\text{Cd}(\text{LTP})_2]_n$ for Improved Enantioseparations on a Chiral Cyclodextrin Stationary Phase in GC. *J. Chromatogr. Sci.* **2016**, *54*, 1467–1474. [[CrossRef](#)] [[PubMed](#)]
118. Zhang, Y.; Wang, L.; Yao, R.-X.; Zhang, X.-M. Fourfold-Interpenetrated MOF $[\text{Ni}(\text{pybz})_2]$ as Coating Material in Gas Chromatographic Capillary Column for Separation. *Inorg. Chem.* **2017**, *56*, 8912–8919. [[CrossRef](#)] [[PubMed](#)]
119. Liu, J.; Wang, F.; Liu, L.-Y.; Zhang, J. Interpenetrated Three-Dimensional Copper–Iodine Cluster-Based Framework with Enantiopure Porphyrin-like Templates. *Inorg. Chem.* **2016**, *55*, 1358–1360. [[CrossRef](#)] [[PubMed](#)]
120. Lang, L.I.; Shengming, X.I.E.; Junhui, Z.; Ling, C.; Pengjing, Z.; Liming, Y. A Gas Chromatographic Stationary of Homochiral Metal-peptide Framework Material and Its Applications. *Chem. Res. Chin. Univ.* **2017**, *33*, 24–30.
121. Zhang, J.; Han, X.; Wu, X.; Liu, Y.; Cui, Y. Multivariate Chiral Covalent Organic Frameworks with Controlled Crystallinity and Stability for Asymmetric Catalysis. *J. Am. Chem. Soc.* **2017**, *139*, 8277–8285. [[CrossRef](#)] [[PubMed](#)]
122. Han, X.; Xia, Q.; Huang, J.; Liu, Y.; Tan, C.; Cui, Y. Chiral Covalent Organic Frameworks with High Chemical Stability for Heterogeneous Asymmetric Catalysis. *J. Am. Chem. Soc.* **2017**, *139*, 8693–8697. [[CrossRef](#)] [[PubMed](#)]
123. Lin, Z.-J.; Lü, J.; Li, L.; Li, H.-F.; Cao, R. Defect porous organic frameworks (dPOFs) as a platform for chiral organocatalysis. *J. Catal.* **2017**, *355*, 131–138. [[CrossRef](#)]



© 2018 by the authors. Licensee MDPI, Basel, Switzerland. This article is an open access article distributed under the terms and conditions of the Creative Commons Attribution (CC BY) license (<http://creativecommons.org/licenses/by/4.0/>).